

AD-758 004

3-D DISPLAY SYSTEM ANALYSIS AND TEST

Herbert C. Towle

Naval Training Equipment Center  
Orlando, Florida

February 1973

DISTRIBUTED BY:

**NTIS**

National Technical Information Service  
U. S. DEPARTMENT OF COMMERCE  
5285 Port Royal Road, Springfield Va. 22151



AD758004

Technical Report: NAVTRAEQUIPCEN IH-187

3-D DISPLAY SYSTEM ANALYSIS AND TEST

Herbert C. Towle

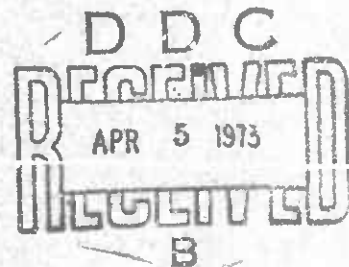
February 1973

Naval Training Equipment Center  
Physical Sciences Laboratory  
Orlando, Florida 32813  
NAVTRAEQUIPCEN TASK No. 1714-05

DOD DISTRIBUTION STATEMENT

Approved for public release;  
distribution unlimited.

Reproduced by  
NATIONAL TECHNICAL  
INFORMATION SERVICE  
U.S. Department of Commerce  
Springfield, VA 22151



NAVAL TRAINING EQUIPMENT CENTER  
ORLANDO, FLORIDA 32813

34 R

## 3-D DISPLAY SYSTEM ANALYSIS AND TEST

## ABSTRACT

This Technical Report presents the results of various analyses and tests conducted at the Naval Training Device Center during the summer of 1970 concerning the 3-D Display System supplied by the Bowles Fluidics Corporation.

The nonlinear differential equation of flow from a fluidic pulse jet motor (FPJM) is presented and solved for the steady state periodic jet velocity caused by a periodic pressure variation. An expression for average FPJM thrust is given as well as a WANG 700 computer program for actual thrust computation.

The depth stability of a submerged model using the Cartesian diver principle was investigated and the differential equation of motion developed. A depth control system was devised and is described.

Thrust measurements were conducted on models using the Bowles supplied hardware. The measurements are in good agreement with the analytical results produced by the WANG 700 computer program.

ACCESSION OF	
NTIS	White Section <input checked="" type="checkbox"/>
DDC	Ref Section <input type="checkbox"/>
MANUSCRIPTS	<input type="checkbox"/>
JUSTIFICATION	
BY	
DISTRIBUTION/AVAILABILITY CODES	
<div style="display: flex; border-bottom: 1px solid black;"> <div style="border-right: 1px solid black; width: 30px; height: 30px; text-align: center; line-height: 30px;">A</div> <div style="width: 30px; height: 30px;"></div> <div style="width: 30px; height: 30px;"></div> </div>	

## GOVERNMENT RIGHTS IN DATA STATEMENT

Reproduction of this publication in whole or in part is permitted for any purpose of the United States Government.

Technical Report: NAVTRAEQUIPCEN IH-187

3-D DISPLAY SYSTEM ANALYSIS AND TEST


Herbert C. Towle

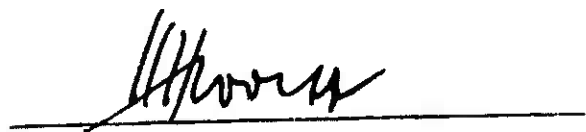
Physical Sciences Laboratory

February 1973

Details of illustrations in this  
document may be better studied  
on microfiche.

Approved:

  
GEORGE DERDERIAN  
Head, Physical Sciences Laboratory

  
DR. H. H. WOLFF  
Technical Director

Naval Training Equipment Center

Orlando, Florida

*Ta*

## DOCUMENT CONTROL DATA - R &amp; D

(Security Classification of title, body of abstract and indexing annotation must be entered when the overall report is classified)

1. ORIGINATING ACTIVITY (Corporate author) Naval Training Equipment Center Orlando, Florida		2a. REPORT SECURITY CLASSIFICATION <b>Unclassified</b>	
		2b. GROUP	
3. REPORT TITLE <b>3-D Display System Analysis and Test</b>			
4. DESCRIPTIVE NOTES (Type of report and include dates) <b>Progress</b>			
5. AUTHOR(S) (First name, middle initial, last name) <b>Herbert C. Towle</b>			
6. REPORT DATE <b>December 1972</b>	7a. TOTAL NO. OF PAGES <b>53</b>	7b. NO. OF REFS <b>3</b>	
8a. CONTRACT OR GRANT NO. <b>RL</b>	9a. ORIGINATOR'S REPORT NUMBER(S) <b>NAVTRAEQUIPCEN IH-187</b>		
8b. PROJECT NO. <b>1714-05</b>	9b. OTHER REPORT NO(S) (Any other numbers that may be assigned this report) <b>None</b>		
10. DISTRIBUTION STATEMENT <b>Approved for public release; distribution unlimited.</b>			
11. SUPPLEMENTARY NOTES		12. SPONSORING MILITARY ACTIVITY <b>Naval Training Equipment Center Physical Sciences Laboratory Orlando, Florida 32813</b>	
13. ABSTRACT <p>This Technical Report presents the results of various analyses and tests conducted at the Naval Training Device Center during the summer of 1970 concerning the 3-D Display System supplied by the Bowles Fluidics Corporation.</p> <p>The nonlinear differential equation of flow from a fluidic pulse jet motor (FPJM) is presented and solved for the steady state periodic jet velocity caused by a periodic pressure variation. An expression for average FPJM thrust is given as well as a WANG 700 computer program for actual thrust computation.</p> <p>The depth stability of a submerged model using the Cartesian diver principle was investigated and the differential equation of motion developed. A depth control system was devised and is described.</p> <p>Thrust measurements were conducted on models using the Bowles supplied hardware. The measurements are in good agreement with the analytic results produced by the WANG 700 computer program.</p>			

DD FORM 1473

(PAGE 1)

S/N 0101-807-6801

UNCLASSIFIED

Security Classification

IL-

UNCLASSIFIED

Security Classification

14. KEY WORDS	LINK A		LINK B		LINK C	
	ROLE	WT	ROLE	WT	ROLE	WT
Depth Control Systems Fluidics Pulsejet Motors Submarines Three Dimensional Display Systems Thrust Measurements						

II

## TABLE OF CONTENTS

<u>Section</u>		<u>Page</u>
I	INTRODUCTION .....	1
II	STATEMENT OF THE PROBLEM .....	7
III	LETTER SYMBOLS .....	8
IV	FLUIDIC PULSE JET MOTOR ANALYSIS .....	10
	4.1 Differential Equation .....	10
	4.2 Resonant Frequency .....	16
	4.3 Approximate Steady-State Solution for Motor Discharge Velocity.....	16
	4.4 Motor Thrust .....	18
V	DEPTH STABILITY OF CARTESIAN DIVER.....	25
	5.1 Description of a Depth Control System (DCS).....	25
	5.2 Analysis of Depth Control System.....	26
VI	SYSTEM MEASUREMENTS .....	31
	6.1 Pressure Variation .....	31
	6.2 Motor Thrust Measurement .....	38
	6.3 Model Velocity .....	38
VII	CONCLUSIONS & SUGGESTIONS FOR FUTURE INVESTIGATIONS .....	40
	REFERENCES .....	42
	APPENDIX A. PROGRAM FOR FLUIDIC PULSE JET MOTOR THRUST...	43

## LIST OF ILLUSTRATIONS

<u>Figure</u>		<u>Page</u>
1	Tank and Model .....	1
2	Tank Cylinder & Piston Hydraulic Actuator .....	2
3	Input Controls .....	3
4	Display Model (Top View) .....	4

# NAVTRAEQUIPCEN IH-187

## LIST OF ILLUSTRATIONS (Continued)

<u>Figure</u>		<u>Page</u>
5	Display Model (Side View) .....	4
6	Sketch of Submarine Model.....	6
7	Fluidic Pulse Jet Motor .....	10
8	Flow Into Chamber .....	13
9	FPJM Equivalent Circuit .....	15
10	Describing Function Approximation for $\frac{1}{1+\frac{4}{\pi} \frac{d}{dt}}$ Nonlinearity .....	16
11	Jet Motor Thrust with Variations In Nozzle Tube Length and Chamber Volume .....	20
12	Jet Motor Thrust with Variations In Pressure Amplitude .....	21
13	Jet Motor Thrust with Variations In Nozzle Tube Diameter and Chamber Volume .....	22
14	Jet Motor Thrust with Variations In Nozzle Tube Length and Diameter .....	23
15	Jet Motor Thrust with Variations In Pressure, Nozzle Tube Diameter, and Chamber Volume .....	24
16	Depth Control System (DCS) for Cartesian Diver .....	25
17	Detail of Region Between Nozzle Tube and Diaphragm .....	26
18	PPJM Thrust, $P_m$ , vs Nozzle Tube Opening $X$ .....	27
19	PITRAN Calibration Set-up .....	31
20	PITRAN Circuit .....	31
21	Tank Vent Pressure (psi) .....	33
22	Hydraulic Pump On. Average Piston Position: 1/2 Stroke. Piston Amplitude: 0.....	34
23	Average Piston Position: 1/2 Stroke. Piston Motion: $\frac{1}{2}$ 0.25 inch. Pressure Variation: 0.12 psi. $f = 10.6$ cycles/sec .....	34



LIST OF ILLUSTRATIONS  
(Continued)

<u>Figure</u>		<u>Page</u>
24	Average Piston Position: 1/2 Stroke. Piston Motion: $\pm 0.5$ inch. Pressure Variation: 0.21 psi. $f = 10.6$ cycles/sec .....	35
25	Average Piston Position: 1/2 Stroke. Piston Motion: $\pm 0.28$ inch. Pressure Variation: $\pm 0.21$ psi. $f = 8$ cycles/sec .....	35
26	Average Piston Position: 1/2 Stroke. Piston Motion: $\pm 0.56$ inch. Pressure Variation: $\pm 0.37$ psi. $f = 8$ cycles/sec .....	36
27	Average Piston Position: 3/4 Stroke (out). Piston Motion: $\pm 0.16$ inch. Pressure Variation: $\pm 0.09$ psi. $f = 8$ cycles/sec .....	36
28	Average Piston Position: 3/4 Stroke (out). Piston Motion: $\pm 0.34$ inch. Pressure Variation: $\pm 0.22$ psi. $f = 8$ cycles/sec .....	37
29	Thrust Model .....	38
30	Thrust & Stability Model .....	41

SECTION I

INTRODUCTION

Initial development of a unique three-dimensional display system, figure 1, was reported in Bowles Fluidics Corporation report, Reference 1, and hardware was delivered to the Naval Training Device Center, Orlando, Florida in May, 1970 under Contract N61339-69-C-0078.

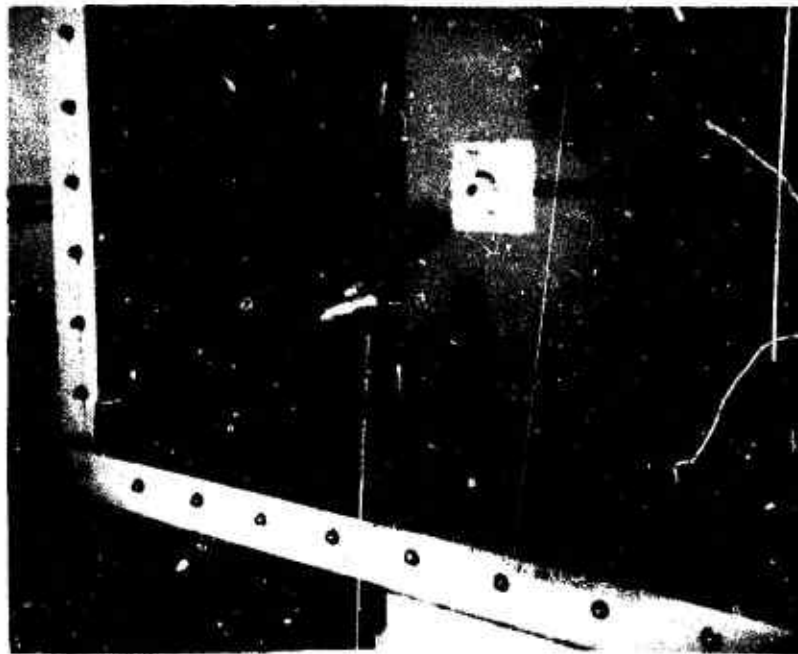


Figure 1. Tank and Model

The system consists of a water filled tank containing a submarine model which moves in three dimensions in response to water pressure variations caused by motion of a hydraulically driven piston in a cylinder located in the side of the tank, figure 1.

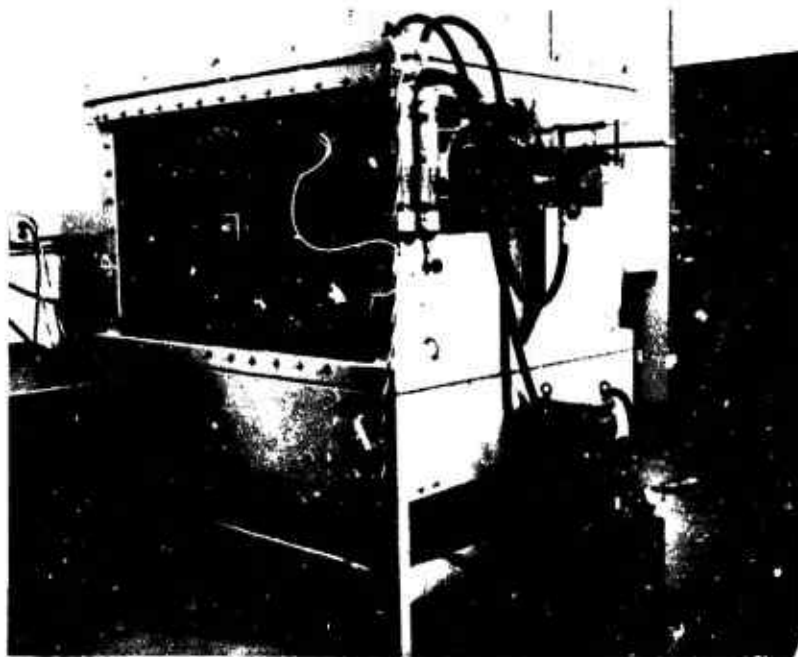


Figure 2. Tank Cylinder & Piston Hydraulic Actuator

Motion of the piston, in turn, is controlled by a feedback system with three inputs: (1) Average position, (2) Amplitude and (3) Frequency of periodic motion, figure 3.

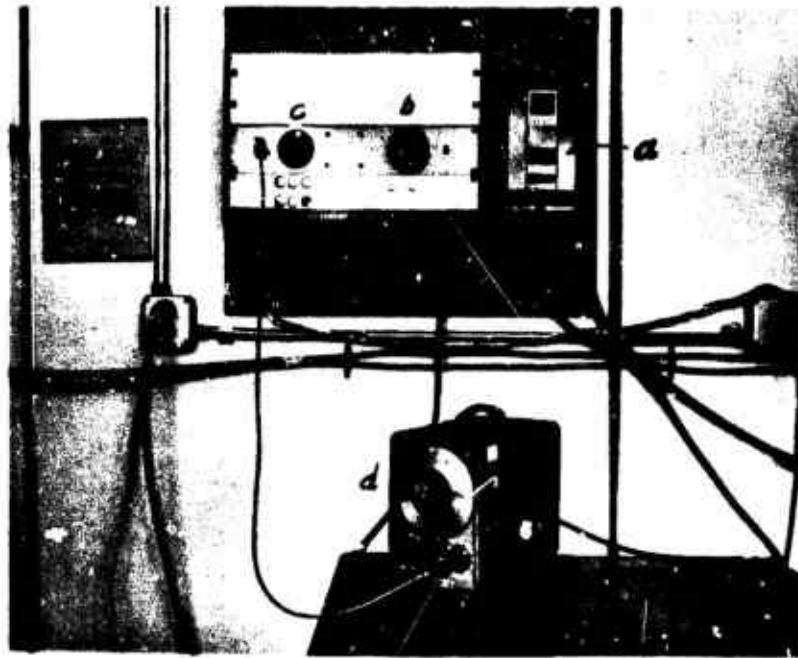


Figure 3. Input Controls

- (a) On-Off Switch
- (b) Average Piston Position (Depth Control)
- (c) Amplitude of Piston Motion (Velocity Control)
- (d) Frequency of Piston Motion (Turning Control)

Vertical position of the model is controlled by the average tank pressure using the principle of the Cartesian diver (devil or imp). A Cartesian diver is a toy consisting of a small figure sealed in a liquid filled tube with vertical position controlled by finger pressure on a diaphragm or cork sealing the top of the tube.

Horizontal velocity of the model is controlled by the amplitude of a periodic tank pressure change, and model turning to the right or left is controlled by the frequency of the periodic pressure change. Model turning is possible because the discharge tube axes, see figures 4 and 5, do not pass through the model center of gravity and any unbalance in flow from the two tubes causes an unbalanced jet thrust which, in turn, provides a turning moment on the model.



Figure 4. Display Model (Top View)

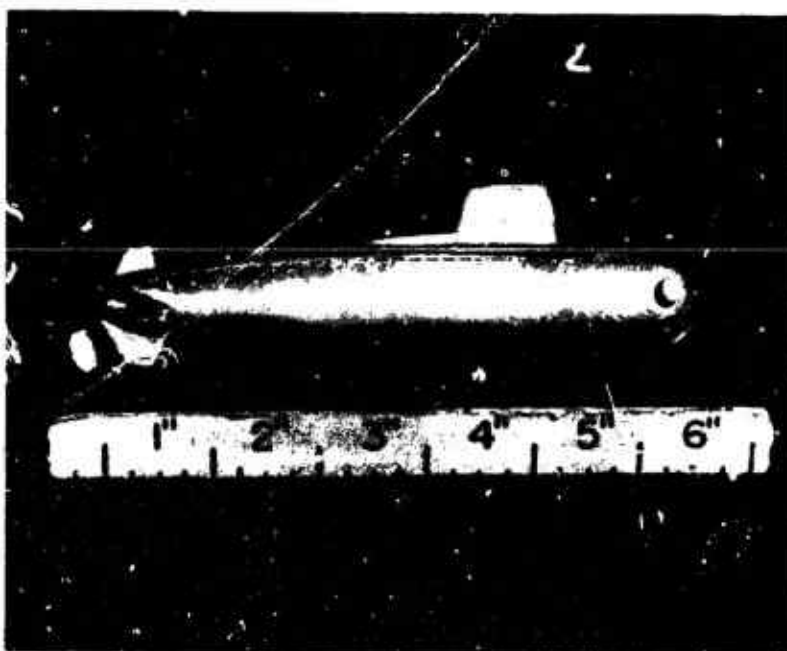


Figure 5. Display Model (Side View)

Control of the relative flow from the two discharge tubes is obtained by adjusting the frequency of the tank pressure variations over a range from the resonant frequency of one tube to the other. For the model shown in figure 4 the maximum right turning moment occurs when the tank pressure is varied at 8 cycles/sec and maximum left turning moment occurs at 11 cycles/sec.

The different resonant frequency for nozzle flow from the two sides depends upon a stiff vertical longitudinal partition which divides the model into a port and starboard side. Each side contains a fixed trapped air volume of 0.4 cubic inches which resonates with the fluid flowing in the corresponding exit tube. The tubes are of sufficiently different lengths to provide the observed difference in resonant frequencies. Figure 6 shows model construction details, and an analysis of the thrust produced by these pulse jet motors is given in Section IV.

The system allows the model to be maneuvered throughout the tank with no visible control devices such as wires or strings and with the desired motion determined solely by means of fluid pressure variations.

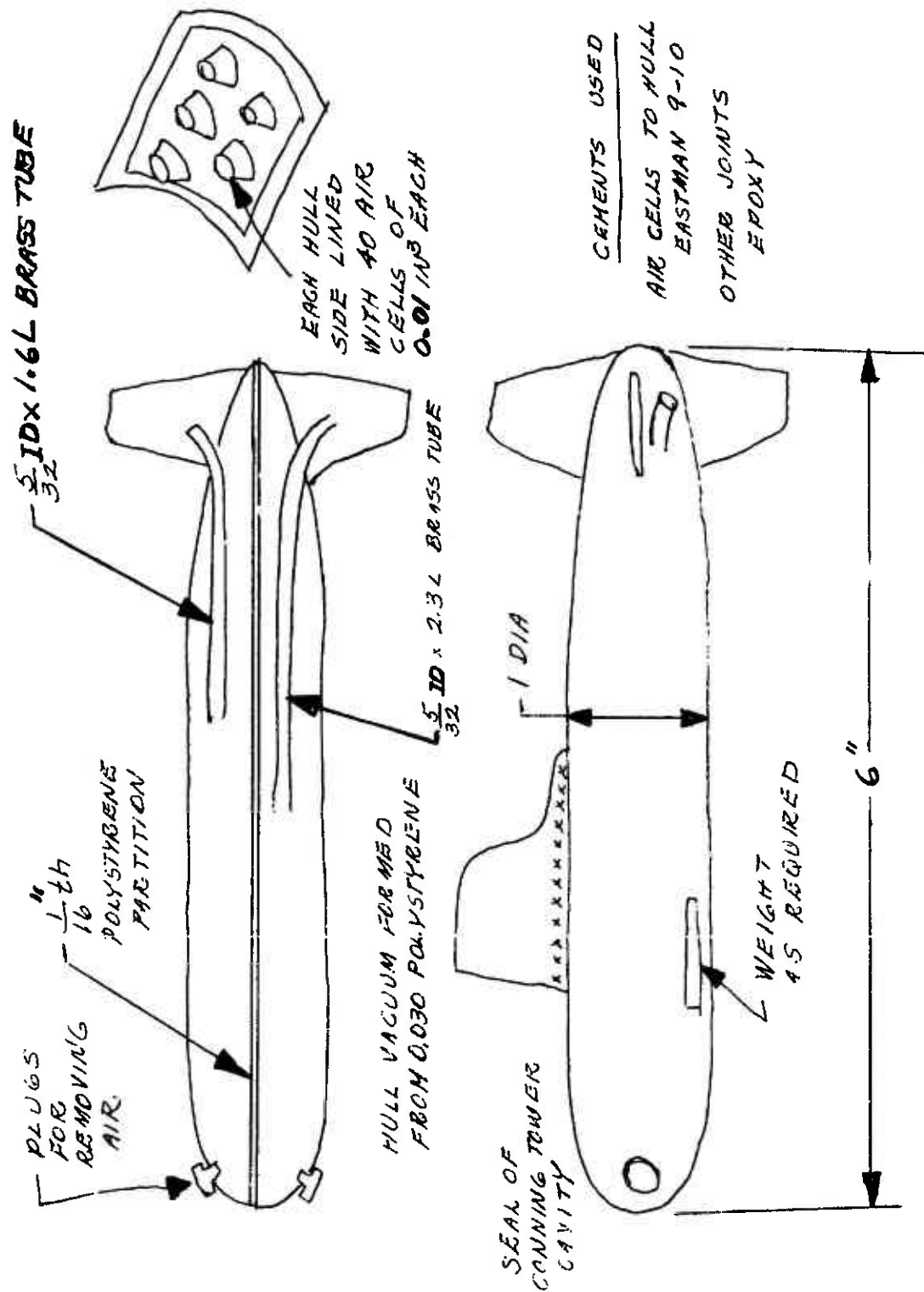


Figure 6. Sketch of Submarine Model

## SECTION II

## STATEMENT OF THE PROBLEM

Control of the display system model by one operator is difficult because the depth control is unstable. An investigation was, therefore, undertaken to establish design criteria for a suitable depth control stabilizing system. It was quickly discovered that the thrust performance analysis for fluidic pulse jet motors as presented in the Bowles report, reference 1, needed to be expanded before it could serve as a basis for a detailed stability analysis. This report presents the results of the thrust and depth stability analyses. Experimental results are given as well as suggestions for future effort. A computer program for the Wang 700A calculator which may be used to compute the thrust of a fluidic pulse jet motor is included as an appendix.



## SECTION III

## LETTER SYMBOLS

- $A$  = nozzle tube flow area,  $\text{in}^2$ .  
 $B$  = viscous damping coefficient,  $\text{lbf-sec/in}$ .  
 $C$  = capacitance, farads (or  $\text{in}^3/\text{lbf.}$ )\*  
 $C_D$  = drag coefficient, dimensionless  
 $d$  = differential operator  
 $D$  or  $D_n$  = nozzle tube diameter,  $\text{in}$ .  
 $D_d$  = effective diameter of diaphragm,  $\text{in}$ .  
 $e$  = electromotive force, volta (or  $\text{lbf/in}^2$ .)\*  
 $f$  = frequency, cycles/sec., or hertz  
 $F$  = thrust,  $\text{lbf}$ .  
 $F_b$  = buoyant force,  $\text{lbf}$ .  
 $F_g$  = force of gravity,  $\text{lbf}$ .  
 $F_m$  = motor thrust,  $\text{lbf}$ .  
 $F_{mm}$  = motor thrust with no nozzle throttling,  $\text{lbf}$ .  
 $F_s$  = shear force due to viscosity,  $\text{lbf}$ .  
 $g$  = acceleration of gravity,  $\text{in/sec}$ .  
 $g_c$  = constant, 386 (numerically equal to standard acceleration of gravity in units of  $\text{in/sec}^2$ )  
 $i$  = current, amperes (or  $\text{in/sec.}$ )\*  
 $j$  =  $\sqrt{-1}$   
 $l$  = nozzle tube length,  $\text{in}$ .  
 $L$  = inductance, henrys (or  $\text{lbm/in}^2$ .)\*  
 $n$  = exponent  
 $N$  =  $R/|U|$   
 $m$  = mass,  $\text{lbm}$ .  
 $o$  = resonant condition - used as subscript

\*Units for analogous mechanical quantities

- $P$  = pressure, lbf/in<sup>2</sup>.  
 $P_{amb}$  = ambient pressure external to model, lbf/in<sup>2</sup>.  
 $P$  = pressure phasor, lbf/in<sup>2</sup>.  
 $q$  = dynamic pressure,  $(1/2) \frac{\rho}{g_c} u^2$ , lbf/in<sup>2</sup>.  
 $Q$  = selectivity  
 $R$  = resistance, ohms (or lbfm/in<sup>2</sup>. - sec.)\*  
 $S$  = surface area of nozzle interior, in<sup>2</sup>.  
 $t$  = time, sec.  
 $T$  = period, sec.  
 $u$  = jet velocity, in/sec.  
 $U$  = velocity phasor, in/sec.  
 $V$  or  $V_a$  = trapped air volume, in<sup>3</sup>.  
 $V_s$  = volume of solid parts of diver, in<sup>3</sup>.  
 $x$  = nozzle opening, in.  
 $\bar{x}$  = average nozzle opening over a period, in.  
 $y$  = vertical dimension, in.  
 $\alpha = 4S V_{ac} F_{mm} / \pi n p_c D_m D_d^2$   
 $\beta = S^2 V_{ac} / n p_c$   
 $\Delta$  = incremental operator  
 $\delta$  = incremental operator  
 $\rho$  = fluid density, lbfm/in<sup>3</sup>.  
 $\omega = 2\pi f$ , angular velocity

## SECTION IV

## FLUIDIC PULSE JET MOTOR

A fluidic pulse jet motor (FPJM) is represented by figure 7. It consists of a chamber with a trapped air space of volume  $V$  and a jet nozzle, shown for simplicity as a symmetrical reentrant tube, of inner diameter  $D$  and length  $\ell$ . When the surrounding ambient fluid pressure is varied periodically, fluid alternately enters and leaves the nozzle. The rate of change of momentum imparted to the fluid causes a reaction force to be developed on the motor. No steady-state rate of change in momentum is imparted to entering fluid since whatever axial velocity is present in the nozzle is destroyed upon impact with the chamber inner surface. Thus, the time average motor thrust may be shown to be proportional to the average momentum of the fluid leaving the motor per unit time. In this respect the motor is the analog of a rectifier in an ac electrical circuit.

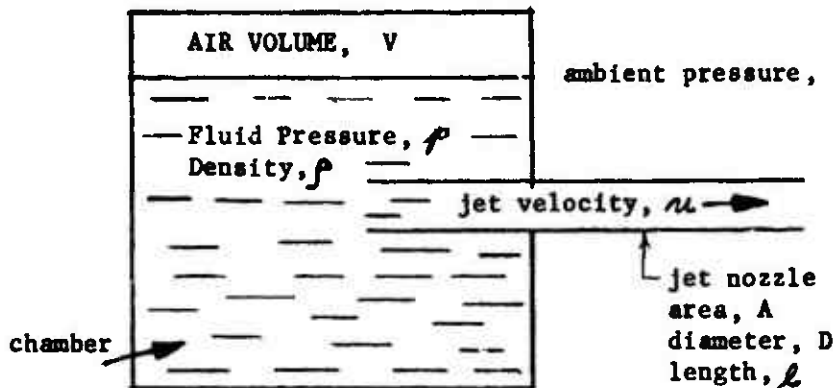


Figure 7. Fluidic Pulse Jet Motor

4.1 Differential Equation

An analysis of a FPJM can be made by direct application of Newton's Law to a free body defined as the material contained within the chamber and nozzle at time  $t$ . Thus, the force,  $F(t)$ , on this free body in the  $u$  direction is

$$F(t) = \frac{1}{g_c} \frac{d}{dt}(mu), \text{ or}$$

$$F(t) = \frac{1}{g_c} \lim_{\Delta t \rightarrow 0} \frac{mu(t + \Delta t) - mu(t)}{\Delta t} \quad (4-1)$$

where  $g_c$  is the appropriate factor of proportionality,  $m$  is mass and  $u$  is fluid axial velocity. The momentum,  $mu$ , at time  $t$  is approximately

$$mu(t) = \rho A l u(t) \quad (4-2)$$

where  $\rho$  is the fluid density and  $A$  and  $l$  are nozzle dimensions shown on figure 7. This relation ignores the axial velocity of the fluid approaching the tube and the over velocity in the "vena contracta". A small constant correction factor could be introduced to account for these effects, if desired, with essentially no change in the analytical results.

There are two cases to consider,  $u > 0$  and  $u < 0$ . The case for  $u > 0$  is treated first. Thus, the momentum at time  $t + \Delta t$  must account for that portion of the free body that has left the nozzle. Since the length,  $\Delta l$ , associated with this portion is approximately  $[u(t) + \frac{1}{2} \frac{du}{dt} \Delta t] \Delta t$ ,

$$\begin{aligned} mu(t + \Delta t) &= \rho A l \left[ u(t) + \frac{du}{dt} \Delta t \right] \quad (\text{momentum in tube}) \\ &+ \rho A \left[ u(t) + \frac{1}{2} \frac{du}{dt} \Delta t \right] \Delta t \left[ u(t) + \frac{1}{2} \frac{du}{dt} \Delta t \right] \\ &\quad (\text{momentum of portion outside nozzle}) \\ &= \rho A \left\{ l u(t) + l \frac{du}{dt} \Delta t + [u(t)]^2 \Delta t \right\} \\ &+ \text{terms of higher order; } u > 0. \end{aligned}$$

From (4-1), therefore,

$$F(t) = \frac{\rho A}{g_c} \left\{ l \frac{du}{dt} + [u(t)]^2 \right\}; \quad u > 0. \quad (4-3)$$

An integration of forces acting on the free body in the  $+u$  direction shows that

$$F(t) = A(p - p_{\text{am}}) - F_s; \quad u > 0, \quad (4-4)$$

where  $p - p_{\text{am}}$  is the difference in static pressure between the motor chamber interior and the surrounding fluid.  $F_s$  is the shear force on the fluid passing through the nozzle which can be expressed in terms of the dynamic pressure,  $q = \frac{1}{2} \frac{\rho}{g_c} u^2$ , as

$$F_n = C_D S q = C_D (\pi D l) \frac{1}{2} \frac{\rho}{g_c} u^2 ; u > 0 \quad (4-5)$$

where  $C_D$  is the drag coefficient and  $S$  is the inner surface area of the nozzle. Since  $A = \frac{\pi}{4} D^2$  equations, (4-3) and (4-4) may be equated giving,

$$p - p_{\text{atm}} = \frac{\rho l}{g_c} \frac{du}{dt} + \frac{\rho u^2}{g_c} \left[ 1 + 2C_D \frac{l}{D} \right] ; u > 0. \quad (4-6)$$

The liquid is considered to be incompressible and, therefore any increase in air volume must cause a corresponding volume of fluid to leave the chamber, or

$$dV = (Au) dt \quad (4-7)$$

In addition, a relation between the chamber pressure,  $p$ , and the air volume,  $V$ , may be written as  $pV^n = \text{a constant}$ , where  $1 \leq n \leq 1.4$ .  $n = 1.0$

for isothermal and  $n = 1.4$  for reversible adiabatic (isentropic) processes. From this relation,

$$\frac{dp}{dt} = -n \frac{p}{V} \frac{dV}{dt} = -n \frac{p}{V} Au \quad (4-8)$$

Differentiating (4-6), while treating  $C_D$  as a constant, and substituting (4-8) yields

$$\frac{\rho l}{g_c} \frac{d^2 u}{dt^2} + \frac{2\rho u}{g_c} \left[ 1 + 2C_D \frac{l}{D} \right] + \frac{mpAu}{V} = - \frac{dp_{\text{atm}}}{dt} \quad (4-9)$$

The case for  $u < 0$  is considered next. The free body under consideration is again the fluid within the chamber and nozzle at time  $t$ .

The portion of the nozzle occupied by the free body at time  $t + \Delta t$  has a length of approximately

$$l + \left( u + \frac{1}{2} \frac{du}{dt} \Delta t \right) \Delta t \approx l + u \Delta t$$

Since  $u < 0$ , this length will be less than  $l$ . At time  $t + \Delta t$  the momentum within the nozzle is

$$mu(t + \Delta t) = \rho A [l + u \Delta t] [u - \frac{du}{dt} \Delta t]$$

This expression is used for the momentum of the free body under consideration and neglects the momentum of the mass in transit between the left hand end of the nozzle and the inner chamber wall. Thus, the total force in the  $+u$  direction is again

$$F = \frac{1}{g_c} \frac{d}{dt} (mu) = \frac{1}{g_c} \lim_{\Delta t \rightarrow 0} \frac{mu(t + \Delta t) - mu(t)}{\Delta t}$$

or

$$F = \frac{1}{g_c} \rho A \left[ l \frac{du}{dt} + u^2 \right] ; u < 0 \quad (4-10)$$

which is identical with (4-3).

The evaluation of the force in terms of pressures and shear force, however, is somewhat more complicated than for the case  $u > 0$ .

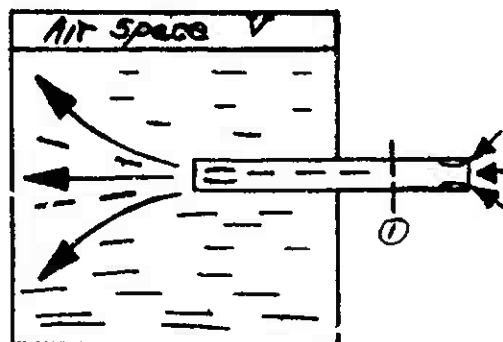


Figure 8. Flow Into Chamber

For  $u < 0$  the jet impact on the inner wall, as shown in figure 8, causes a local impact over-pressure of an amount  $\delta p$  above the chamber pressure  $p$ . Since there is no net axial force developed by the motor when  $u < 0$  and  $\frac{du}{dt} = 0$ , i.e., steady state, the integral of the over-pressure may be shown to be equal to the momentum flow divided by  $g_c$ , or

$$\int_{Wall} \delta p dA = \frac{\rho A u^2}{g_c} ; \frac{du}{dt} = 0.$$

The mass of the fluid moving axially between the nozzle and the inner chamber is small and the jet transit time within the chamber is considered negligible. Consequently, this expression is used for the integrated over-pressure, even in case  $du/dt \neq 0$ . Thus, letting  $p_1$  represent the pressure within the nozzle at the edge of the free body at time  $t+\Delta t$  (see figure 8) an expression for  $F$  in the  $+u$  direction is

$$F = (p - p_1)A + \int_{w.c.} \delta p dA + C_D S q$$

$$= (p - p_1)A + \frac{\rho S u^2}{g_c} + C_D S \frac{\rho u^2}{2g_c}$$

The vena contracts at the inlet causes an inlet pressure loss, and from any text on hydraulics it is found that

$$p_1 = p_{\text{am}} - \frac{\rho u^2}{g_c}$$

or

$$F = (p - p_{\text{am}})A + \frac{2\rho A}{g_c} \left[ 1 + C_D \frac{l}{D} \right] u^2; u < 0. \quad (4-11)$$

Thus from (4-10) and (4-11)

$$p - p_{\text{am}} = \frac{\rho l}{g_c} \frac{du}{dt} - \frac{\rho}{g_c} \left[ 1 + 2C_D \frac{l}{D} \right] u^2; u < 0. \quad (4-12)$$

Differentiation of (4-12) and using (4-8),

$$\frac{\rho l}{g_c} \frac{d^2 u}{dt^2} - \frac{2\rho u}{g_c} \left[ 1 + 2C_D \frac{l}{D} \right] \frac{du}{dt} + \frac{m p A u}{V} = \frac{d p_{\text{am}}}{dt}; u < 0. \quad (4-13)$$

Equations (4-9) and (4-13) may be combined and written as

$$\frac{\rho l}{g_c} \frac{d^2 u}{dt^2} + \frac{2\rho |u|}{g_c} \left[ 1 + 2C_D \frac{l}{D} \right] \frac{du}{dt} + \frac{m p A u}{V} = \frac{d p_{\text{am}}}{dt} \quad (4-14)$$

without restriction on the sign of  $u$ . The  $|u|$  factor in the second term causes the system to be nonlinear and not subject a simple linear analysis of a second order system. Note also that a change in sign of  $u$  results in the change in sign of all terms on the left hand side of (4-14). This is to be expected since the nozzle is symmetric and a reverse of the pressure driving force must reverse the flow.

An analogous relation to (4-14) for a series R, L, C electric circuit is

$$L \frac{d^2 i}{dt^2} + R \frac{di}{dt} + \frac{1}{C} i = \frac{de}{dt} \quad (4-15)$$

where

L = inductance, henrys

i = current, amperes

R = resistance, ohms

C = capacitance, farads

e = electromotive force, volts

The FPJM can, therefore, be considered to be the analog of the nonlinear equivalent circuit shown in Figure 9.

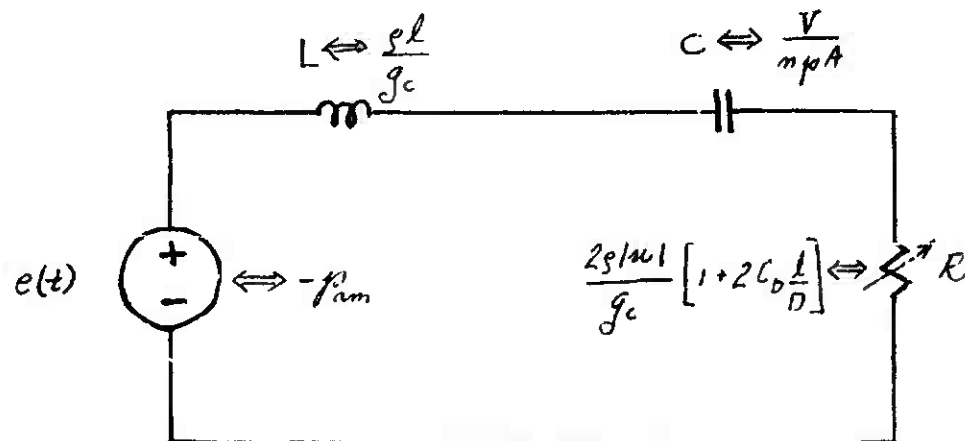


Figure 9. FPJM Equivalent Circuit



#### 4.2 Resonant Frequency

While an exact analysis of the nonlinear system of equation (4-14) or figure 9 is rather involved, the resonant frequency,  $f_c$ , for the limiting case of  $R = 0$  may be easily obtained as

$$f_c = \frac{1}{2\pi \sqrt{LC}} = \frac{1}{4} \sqrt{\frac{g_c n p}{\pi \rho l V}} D \quad (4-16)$$

Using  $g_c = 32.17 \cdot 12 = 386$

$$\rho = 62.4 \left( \frac{\text{lbm}}{\text{ft}^3} \right) \cdot \frac{1}{1728} \left( \frac{\text{ft}^3}{\text{in}^3} \right) = 0.0361 \text{ lbm/in}^3$$

$n = 1.4$ , for an isentropic process

$p = 14.7 \text{ lbf/in}^2$ ,

This expression becomes

$$f_c = 66.16 \frac{D}{\sqrt{LV}} = 2\pi \omega_c$$

with units:

$D$  (inches),  $L$  (inches),  $V$  (cubic inches) and  $f$  (hertz = cycles per second).

#### 4.3 Approximate Steady-State Solution for Motor Discharge Velocity

An approximate solution for the second order nonlinear differential equation, 4-14, can be obtained by using the describing function as discussed by Kochenburger, ref. 2. With this technique the input-output relation for the nonlinearity may be approximated as shown in figure 10.

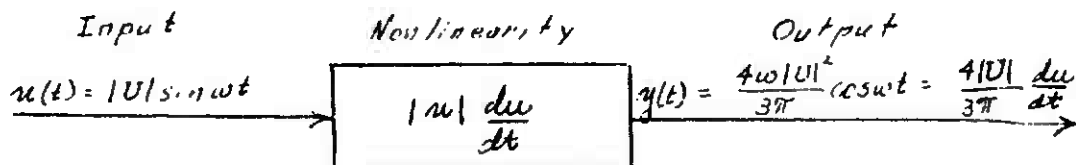


Figure 10. Describing Function Approximation for  $|u| \frac{du}{dt}$  Nonlinearity

Using this approach, all harmonics of the output which are of higher order than the first are neglected. If the pressure,  $p_{am}$ , contains a sinusoidal variation about an average value, the fundamental component of the nozzle discharge velocity will vary at the same frequency,  $f = \omega/2\pi$ . Thus, representing the amplitude of the velocity variation by  $|U|$ ,

$$u = |U| \sin \omega t$$

And equation (4-14) may be used to find the  $df_{am}/dt$  required. A particularly convenient method of solution uses phasors and in this notation, along with the describing function approximation, equation (4-14) has the steady-state solution

$$\left\{ -\frac{\rho l \omega^2}{g_c} + j \frac{8 \rho \omega |U|}{3 \pi g_c} \left[ 1 + 2 C_D \frac{l}{D} \right] + \frac{\pi p A}{V} \right\} U = j \omega P \quad (4-17)$$

or

$$U = \frac{-P}{\frac{8 \rho |U| [1 + C_D \frac{l}{D}]}{3 \pi g_c} + j \left[ \frac{\rho l \omega}{g_c} - \frac{\pi p A}{V \omega} \right]} \quad (4-18)$$

where  $j = \sqrt{-1}$  and upper case U and P are velocity and pressure phasors.

The corresponding phasor equation for the analogous electric circuit is

$$I = \frac{E}{Z} = \frac{E}{R + j \left[ \omega L - \frac{1}{\omega C} \right]} \quad (4-19)$$

The describing function approach, therefore, allows the identification of a simpler expression for

$$R_{eq} = \frac{8 \rho |U| \left[ 1 + 2 C_D \frac{l}{D} \right]}{3 \pi g_c} \quad (4-20)$$

Note that the equivalent L and C are unchanged from those identified in figure 9. From (4-20) it is seen that the equivalent resistance is proportional to the amplitude of U. Thus, the circuit selectivity or Q, where

$$Q = \frac{\omega_c L}{R} = \frac{3 \pi \omega_c l}{8 |U| \left[ 1 + C_D \left( \frac{l}{D} \right) \right]} \quad (4-21)$$

Evidently, for a fixed natural frequency,  $\omega_c$ , the Q of the motor varies directly with  $\ell$  (for  $2C_D \frac{\ell}{D} \ll 1$ ) and inversely with the velocity amplitude.

At resonance  $\omega L = 1/\omega C$  and the current from (4-19) depends only upon the circuit R. Analogously, the motor the jet velocity at resonance,  $U_0$ , depends only on  $R_{eq}$  and from (4-20)

$$U_c = \frac{-3\pi g_c |P|}{8\gamma |U| [1 + 2C_D \frac{\ell}{D}]}$$

or

$$|U_c| = \sqrt{\frac{3\pi g_c |P|}{8\gamma [1 + 2C_D \frac{\ell}{D}]}} \quad (4-22)$$

Thus, the describing function approach yields simple expressions for the selectivity, Q, and jet velocity of a FPJM at resonance.

#### 4.4 Motor Thrust

The average net thrust of the motor at any general frequency,  $f$ , is equal to the average value of the momentum flow leaving the device for a period,  $T = 1/f$ . Thus

$$F_{avg} = \frac{1}{T} \int_t^{t+T} \frac{\rho A [u(t)]^2}{g_c} dt ; u(t) > 0, \quad (4-23)$$

or considering only the fundamental component of  $u(t)$ ,

$$F_{avg} = \frac{\rho A}{g_c} \frac{|U|^2}{4} \quad (4-24)$$

At resonance, using (4-22)

$$F_{avg,c} = \frac{3\pi A |P|}{32 [1 + C_D \frac{\ell}{D}]} \quad (4-25)$$

The thrust at frequencies other than resonance can be obtained by solving (4-18) for  $|U|^2$ . First  $N$  is defined as

$$N \triangleq \frac{8\gamma}{3\pi g_c} \left[ 1 + C_D \frac{\ell}{D} \right] = \frac{R_{eq}}{|U|} \quad (4-26)$$

Then from (4-18)

$$|U|^2 = \frac{|P|^2}{N^2 |U|^2 + \left[ \omega L - \frac{1}{\omega C} \right]^2} \quad (4-27)$$

or

$$N^2 \left[ |U|^2 \right]^2 + \left[ \omega L - \frac{1}{\omega C} \right]^2 |U|^2 - |P|^2 = 0 \quad (4-28)$$

Equation (4-28) may be solved for  $|U|^2$  from the quadratic formula using the + sign on the radical term since  $|U|^2$  must always be positive. The average thrust is then given by (4-24). A program (Appendix A) was written for the Wang 700 which provides rapid solutions for thrust as a function of motor volume,  $V$ , nozzle diameter,  $D$ , nozzle length,  $l$ , and amplitude of the sinusoidal external pressure variation,  $P$ . The program is based on water with a density of  $62.4 \text{ lbm/ft}^3$ ,  $C_D = 0.01$ , an average motor chamber pressure of  $14.7 \text{ lbf/in}^2$  and  $n = 1.4$  for isentropic changes in air volume. Figures 11 through 14 show the variation of thrust as a function of frequency with different combinations of parameters held constant such that the undamped natural frequency,  $f_0 = 10 \text{ cycles/sec}$ . Figure 15 gives the calculated performance of the port and starboard motors of the submarine model shown in figure 6.

FLUIDIC PULSE JET MOTORCALCULATED THRUSTPressure Variation Amplitude,  $P = 0.2$  psiNozzle Tube Diameter,  $D = 0.117$  in.Curve Parameters:Nozzle Tube Length,  $L$ , in.Chamber Volume,  $V$ , in.<sup>3</sup>

Parameter	
$L$	$V$
0.25	2.4
1.0	0.6
3.0	0.2

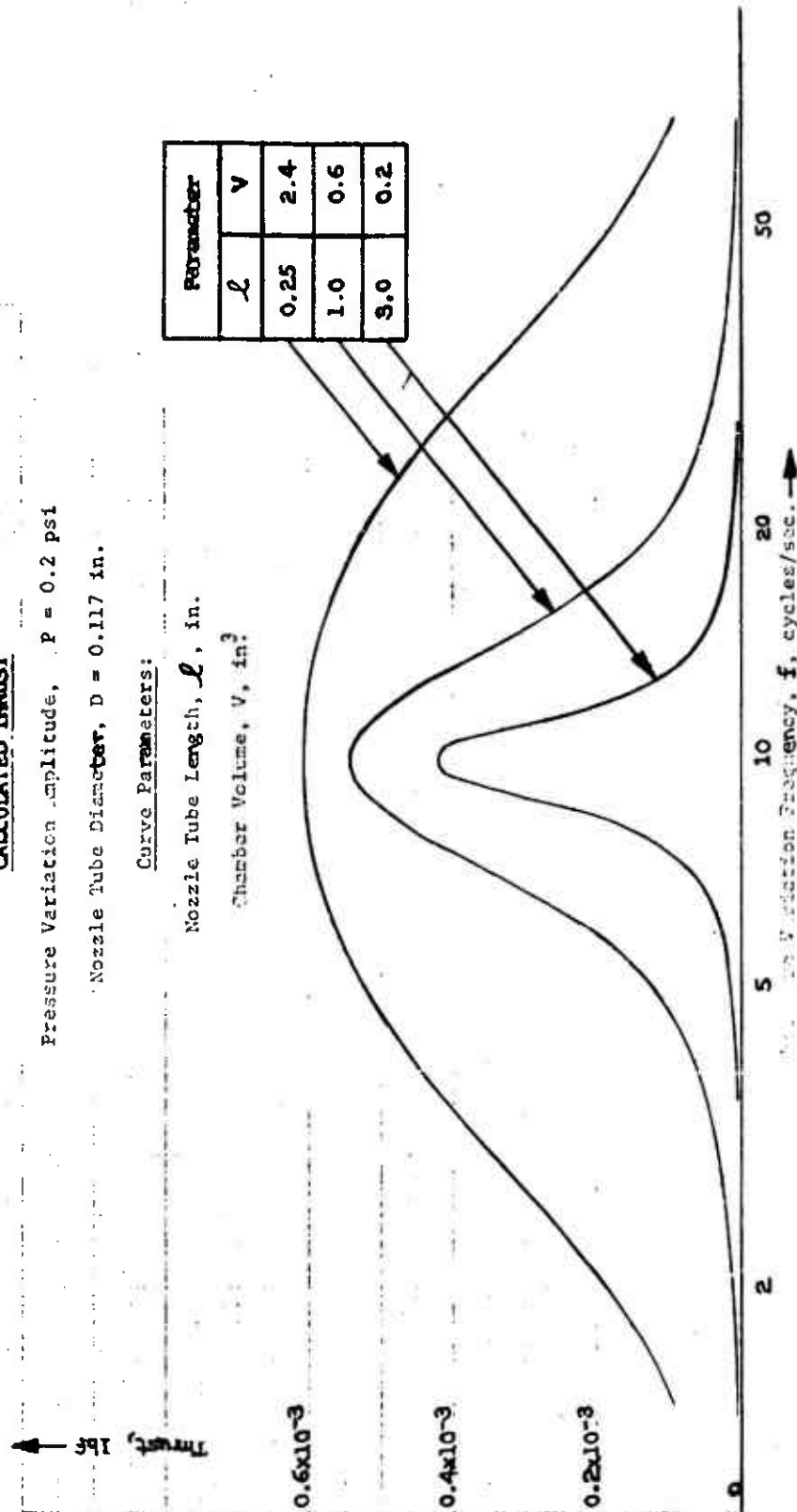


Figure 11. Jet Motor Thrust with Variations in Nozzle Tube Length and Chamber Volume

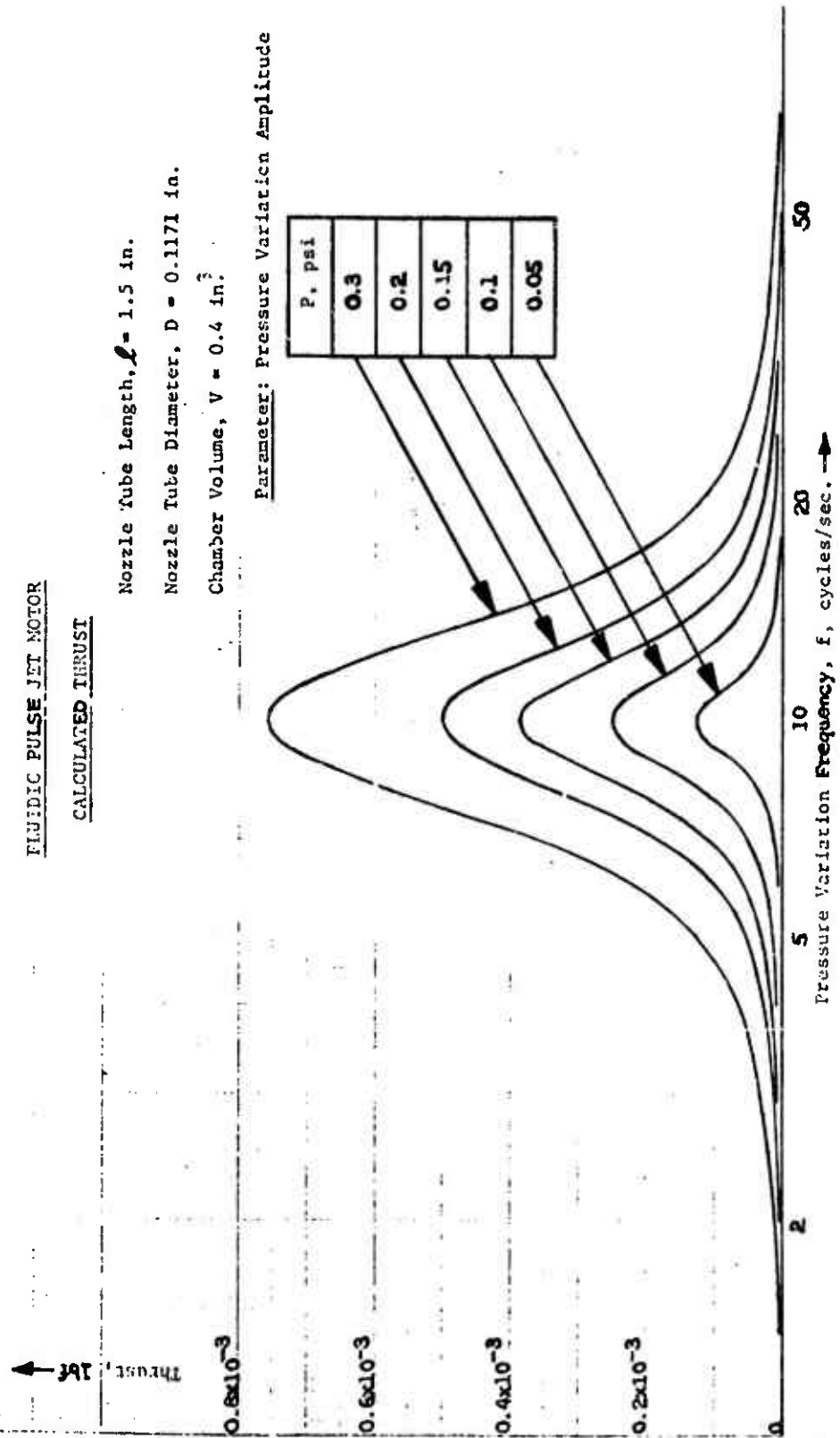
FLUIDIC PULSE JET MOTORCALCULATED THRUSTNozzle Tube Length,  $l = 1.5$  in.Nozzle Tube Diameter,  $D = 0.1171$  in.Chamber Volume,  $V = 0.4$  in.<sup>3</sup>Parameter: Pressure Variation Amplitude

Figure 12. Jet Motor Thrust with Variations in Pressure Amplitude

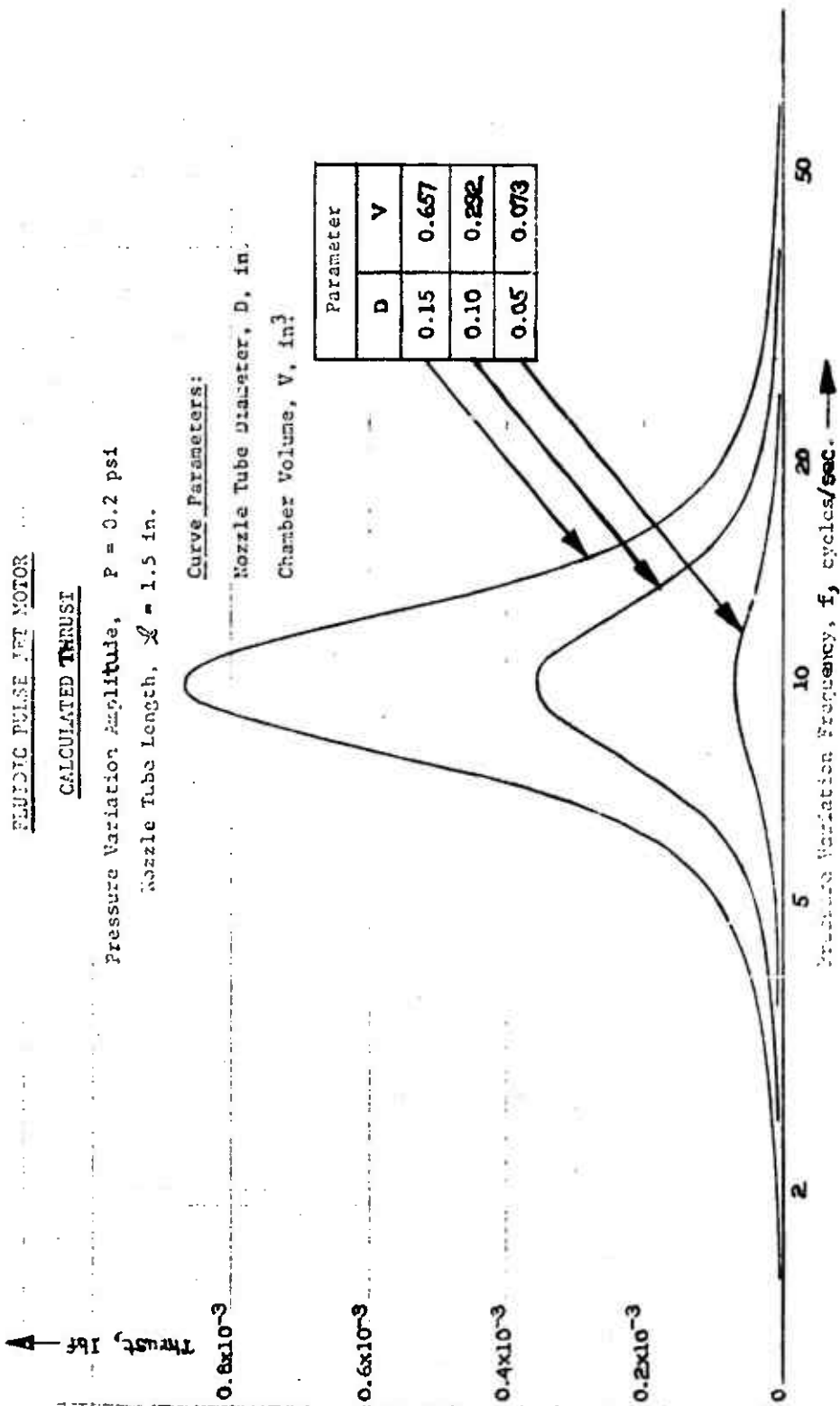


Figure 13. Jet Motor Thrust with Variations in Nozzle Tube Diameter and Chamber Volume

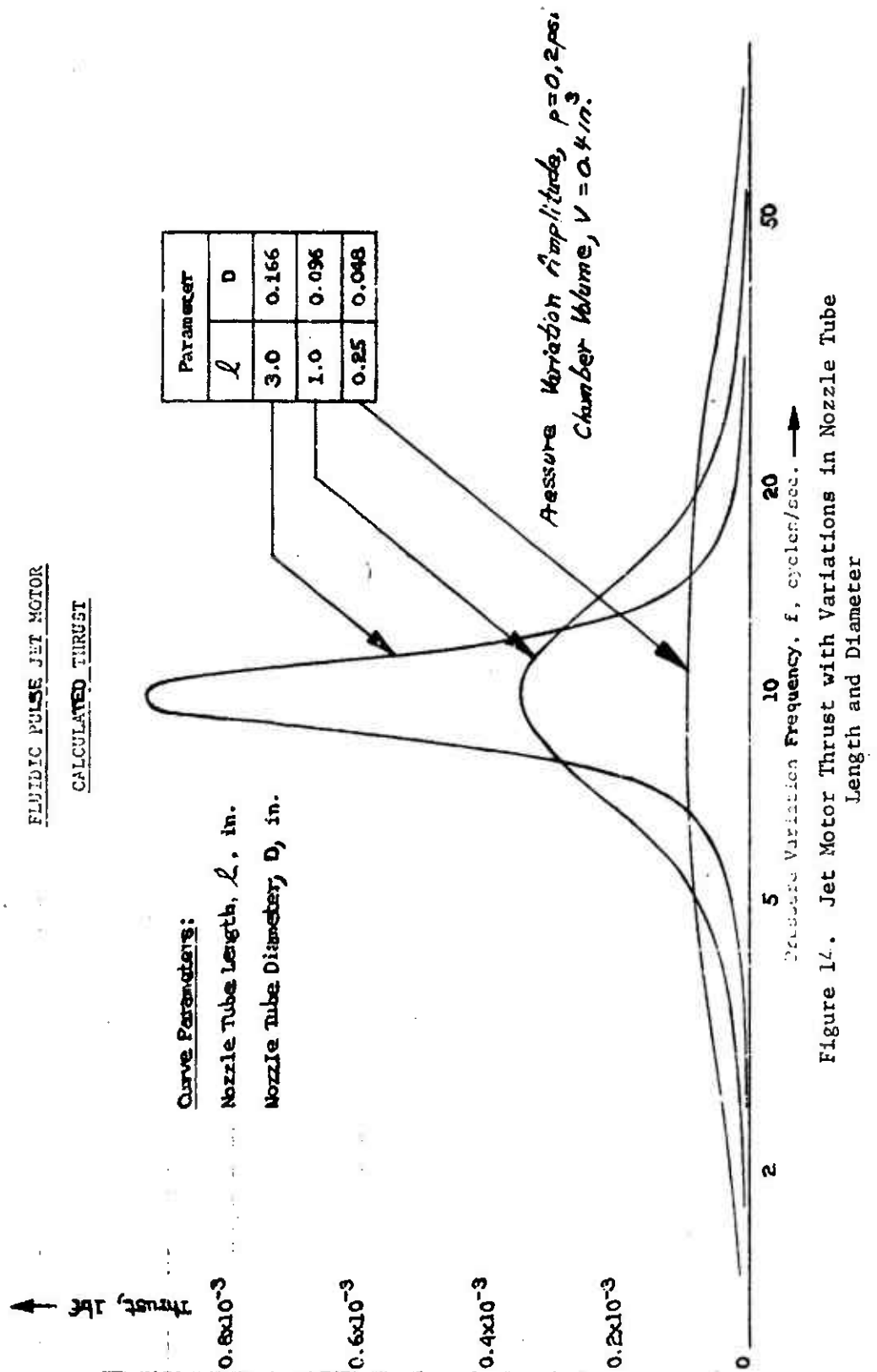


Figure 14. Jet Motor Thrust with Variations in Nozzle Tube Length and Diameter



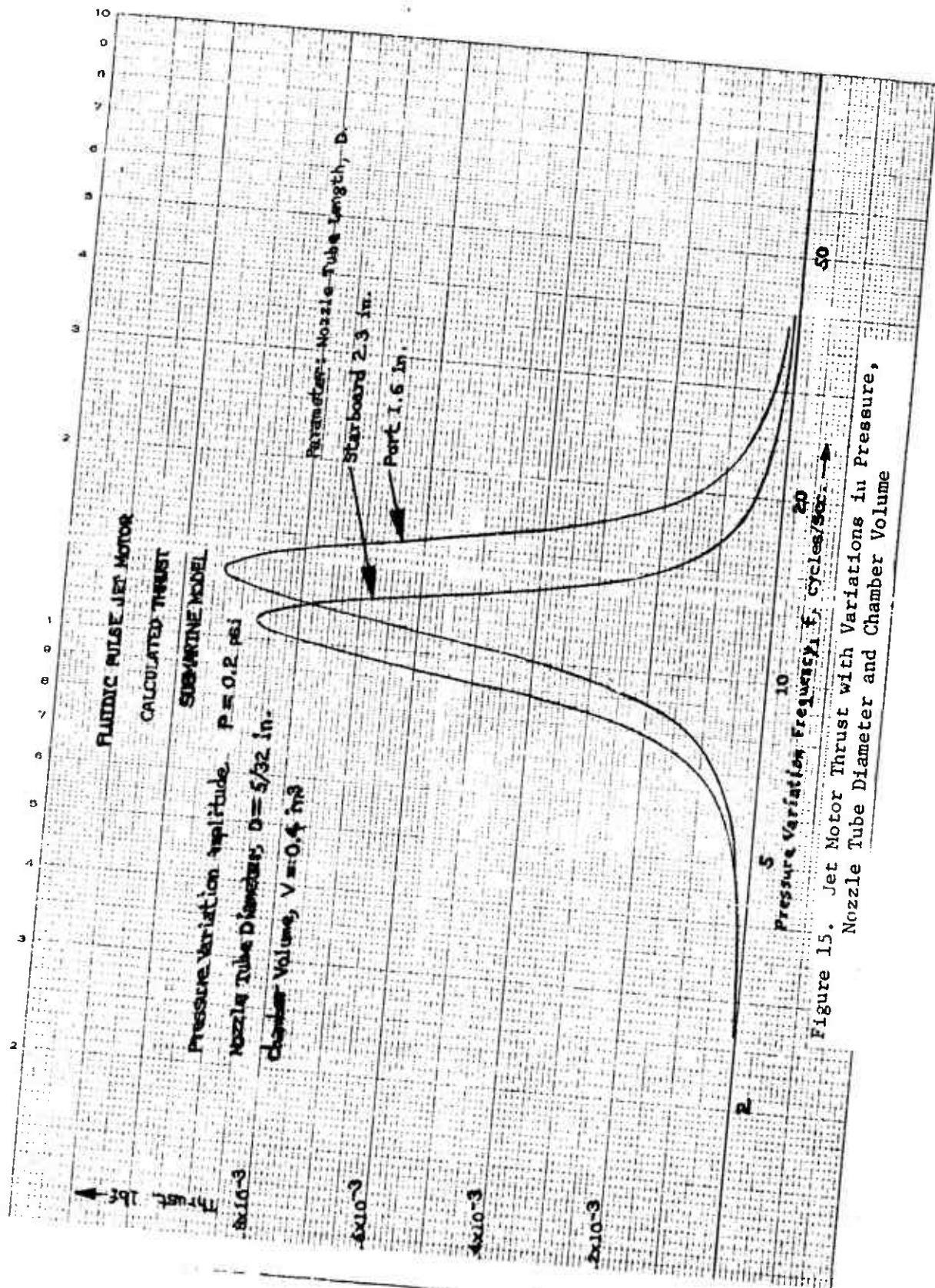


Figure 15. Jet Motor Thrust with Variations in Pressure, Nozzle Tube Diameter and Chamber Volume

## SECTION V

DEPTH STABILITY OF CARTESIAN DIVER

A simple Cartesian Diver has an equilibrium point at a depth determined by the amount of trapped air and the mass of the device. This equilibrium point, however, is unstable whenever it exists between the upper and lower surfaces of the tank containing the diver. Thus, if the diver position is perturbed either upward or downward from such a point, a force is developed in a direction to increase the perturbation. If, for example, the device is forced below the equilibrium point, the hydrostatic pressure on the trapped air becomes higher, the air volume becomes smaller, buoyancy decreases and the device tends to sink further, provided no correction force is applied. Such a correction force can be furnished by reducing the pressure of the surrounding fluid as in the case of the familiar toy. Alternatively, a corrective vertical jet force can be controlled by a suitable sensing element within the diver. One such possible control device is shown in figure 16 and described in the following section.

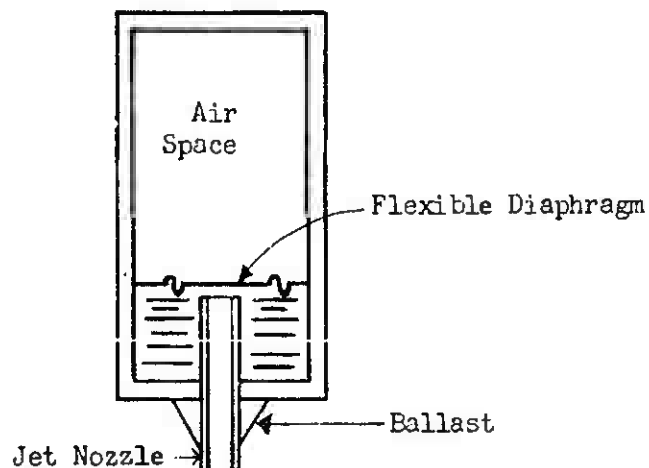
5.1 Description of a Depth Control System (DCS)

Figure 16. Depth Control System (DCS) for Cartesian Diver

Operation of the depth control system (DCS) of figure 16 is accomplished by throttling the nozzle of a fluidic pulse jet motor (FPJM) with a flexible diaphragm. Assume that the fluid surrounding the diver is pulsating about some fixed average value and that the diver is at the equilibrium point. This insures that there is an equality between the downward gravity force on the diver and the sum of the upward forces due to both the buoyance of the air space and the FPJM average thrust. When the diver position is perturbed downward there is again an increase in average pressure on the air space and a decrease in buoyancy due to the resulting reduction in air volume. With the DCS in operation, however, the decrease in air volume results in an opening of the passage between the top of the FPJM nozzle tube and the flexible diaphragm which increases the vertical jet thrust. When this increase in jet thrust is greater than the loss of buoyancy, there will be a net corrective force tending to eliminate the initial downward position perturbation. It is also easy to see that a downward corrective force will arise if the initial position perturbation from equilibrium is upward.

Quantitative design requirements to insure that a DCS will provide a stable equilibrium are developed in the next section of the report.

## 5.2 Analysis of Depth Control System

The DCS for the Cartesian Diver shown in figure 16 may be analyzed by first considering the region between the nozzle tube and the flexible diaphragm. Figure 17 shows the diaphragm and the upper end of the nozzle separated by a distance  $x$ . It is assumed that the pressure in the tank containing the diver is pulsating sinusoidally with a fixed frequency and amplitude about an average value and that equilibrium is obtained when the time-average value of  $x$ , designated by  $\bar{x}$ , is equal to  $x_0$ .

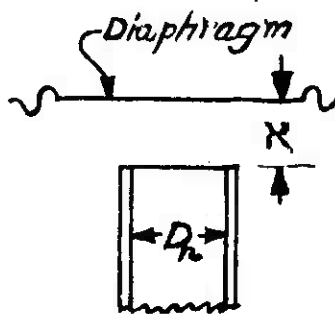


Figure 17.

Detail of Region Between Nozzle Tube  
and Diaphragm

It is also assumed that the upward jet thrust on the diver caused by the pulsating flow leaving the nozzle monotonically increases with increasing  $\bar{x}$ . When  $\bar{x} = 0$ , no flow can pass through the nozzle and thus no upward thrust results. As  $\bar{x}$  increases from zero, the upward thrust increases until until  $\bar{x}$  reaches a value comparable to the nozzle inner diameter when the diaphragm provides essentially no nozzle throttling and the FPJM thrust approximates the value,  $F_{mm}$ , calculated by the method described in Section 4.4. Although an exact formulation of the relation between the opening,  $\bar{x}$ , and the upward motor thrust,  $F_m$  is not available, it is expected to appear as shown in figure 18.

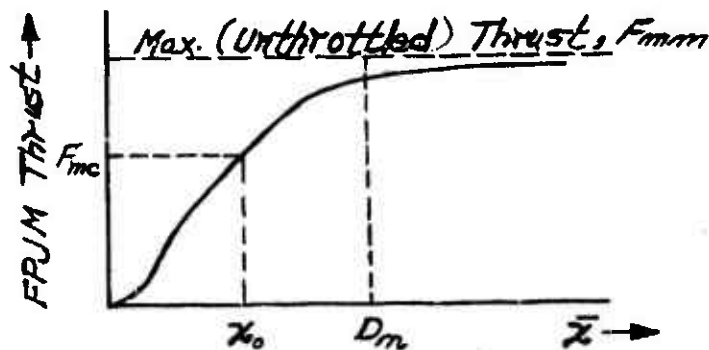


Figure 18. FPJM Thrust,  $F_m$ , vs Nozzle Tube Opening  $\bar{x}$ . ( $D_m$  is the nozzle inner diameter,  $x_0$  is the opening at equilibrium and  $F_{m0}$  is the corresponding thrust).

At the equilibrium point the total net time-average vertical force in the  $+\bar{y}$  direction (upward) must be zero. Three such forces act on the diver, the downward force of gravity, the upward fluidic pulse jet motor (FPJM) thrust and the upward buoyant force equal to the weight of the displaced liquid. The latter two forces have both, (1) a periodic component with the same frequency as the external pressure variation and a mean value of zero and, (2) a longer term "average value" about which the periodic component varies. The periodic component of these forces causes a small amplitude periodic motion of the diver to be superimposed on the motion caused longer term changes in average force values. The small periodic effects are neglected in the following analysis and attention is concentrated on the longer term effects caused by changes in average values of forces and diver position,  $y$ .

Expressions relating the average values of the vertical forces and position of a diver may be derived by considering upward values as positive. Thus the force of gravity,  $F_g$ , is

$$F_g(\text{lbf}) = - \frac{g(\text{in./sec.}^2)}{g_0(\text{ft./sec.}^2)} \cdot m(\text{lbm})$$

The buoyant force,  $F_b$ , depends on the total volume of displaced fluid,  $V_s + V_a$ , where  $V_s$  is the volume of the solid parts of the diver and  $V_a$  is the air volume. Thus

$$F_b = (V_s + V_a) (\text{m}^3) \frac{g (\text{m/sec}^2)}{g_0 (\text{dimensionless})} \rho (\text{kg/m}^3)$$

Letting  $F_m$  represent the FPJM thrust and using the subscript "o" to indicate equilibrium conditions,

$$F_g + F_b + F_m = 0 \quad (5-1)$$

or, since  $g/g_0$  has a numerical value of 1 at sea-level

$$-m + \rho V_s + \rho V_a + F_{m0} = 0 \quad (5-2)$$

When the diver is perturbed from the equilibrium depth,  $y_0$ , by an amount  $\delta y$ , the gravit. force is unchanged. However, the average FPJM thrust will change to

$$F_m(y_0 + \delta y) = F_{m0} + \frac{dF_m}{dy} \delta y = F_{m0} + \left( \frac{dF_m}{d\bar{x}} \right) \left( \frac{d\bar{x}}{dy} \right) \delta y \quad (5-3)$$

A reasonable value for  $\frac{dF_m}{d\bar{x}}$  may be obtained by considering that the thrust changes from zero to full value,  $F_{mm}$ , as  $\bar{x}$  changes from zero to  $D_n$  or as an approximation,

$$\frac{dF_m}{d\bar{x}} = \frac{F_{mm}}{D_n} \quad (5-4)$$

Letting  $D_d$  be the effective diameter of the diaphragm shown in figure 5-1, the time average change in volume,  $dV_a$ , of the airspace is

$$dV_a = - \frac{\pi}{4} (D_d)^2 d\bar{x} \quad (5-5)$$

From the usual expression for the air volume

$$p V_a^n = \text{a constant} = p_0 V_{a0}^n,$$

$$dV_a = - \frac{V_{a0}}{n p_0} d\bar{p}, \quad (5-6)$$

where the bar over the symbol  $p$  again denotes a time average.

From the hydrostatic relation,

$$d\bar{p} = -\rho dy. \quad (5-7)$$

Thus 
$$\frac{d\bar{p}}{dy} = - \frac{4 \rho V_{a0}}{\pi n p_0 D_1^2}$$

and from equation (5-3)

$$\frac{dF_m}{dy} = - \frac{4 \rho V_{a0} F_{m0}}{\pi n p_0 D_m D_1^2} \triangleq -\alpha. \quad (5-8)$$

Note that equation (5-8) defines the constant  $\alpha$ ,

and

$$F_m(y_0 + \delta y) = F_{m0} - \alpha \delta y. \quad (5-9)$$

Letting  $F_b(y)$  represent the buoyant force

$$F_b(y_0 + \delta y) = F_{b0} + \left( \frac{dF_b}{dy} \right) \delta y$$

where

$$\frac{dF_b}{dy} = \rho \left[ \frac{dV_a}{dy} + \frac{dV_c}{dy} \right]$$

or

$$\frac{dF_b}{dy} = \rho \frac{dV_a}{dy} = \rho \frac{dV_a}{d\bar{p}} \frac{d\bar{p}}{dy}.$$

Use of relations (5-6) and (5-7) shows that

$$\frac{dF_b}{dy} = \frac{\rho^2 V_{a0}}{n p_0} \triangleq \beta \quad (5-10)$$

which defines the quantity  $\beta$ . Thus

$$F_b(y_c + \delta y) = F_{bc} + \beta \delta y. \quad (5-11)$$

Assuming a viscous drag force of an amount  $-B \frac{dy}{dt}$ , the differential equation of motion for small changes from equilibrium becomes

$$\frac{m}{g_c} \frac{d^2 y}{dt^2} = -B \frac{dy}{dt} + F_g + F_{bc} + \beta \delta y + F_{mc} - \alpha \delta y \quad (5-12)$$

The value for "m" used in this relation must include any liquid within the diver that will be accelerated along with the actual structure of the device. Because of (5-1) the equilibrium terms in (5-12) may be eliminated and this relation rewritten as

$$\left[ \frac{m}{g_c} \frac{d^2}{dt^2} + B \frac{d}{dt} + (\alpha - \beta) \right] \delta y = 0 \quad (5-13)$$

For stability, all coefficients in this expression must be positive. Thus, it is necessary that

$$\alpha > \beta$$

Or, from (5-8) and (5-10)

$$F_{mm} > \frac{\pi}{4} \rho D_n D_d^2 \quad (5-14)$$

Relation (5-14) states the requirement for depth stability of a diver with a FPJM DCS. As noted in the analysis it is based on an approximation for the variation of FPJM thrust with diaphragm-nozzle opening. It should also be observed that  $D_d$ , the effective diameter of the diaphragm, is actually defined by equation (5-5) through the relation between air space volume  $V_a$ , and diaphragm-nozzle opening  $\bar{x}$ .  $D_d$  may, therefore, be difficult to compute for a given design. In view of these facts, relation (5-14) must be considered more of a guide indicating the important factors for stable operation rather than a go-no-go design criterion. The relation, for example, indicates that as the amplitude of pressure pulsation increases from zero and thrust,  $F_{mm}$ , increases a value will be reached for which depth stability is first attained. Stability will then be maintained for higher pressure amplitudes at the same pulsation frequency. The relation also indicates the desirability of a small effective diaphragm diameter which is equivalent to a large diaphragm movement for a given change in fluid pressure.

## SECTION VI

## SYSTEM MEASUREMENTS

This section describes measurements made of tank pressure variation, motor thrust and submarine velocity.

6.1 Pressure Variation

Tank pressures were measured using a pressure sensitive transistor (PITRAN) made by Stow-Laboratories, Inc. The PITRAN was mounted in the tank hatch and calibrated against a water filled manometer as in figure 19.

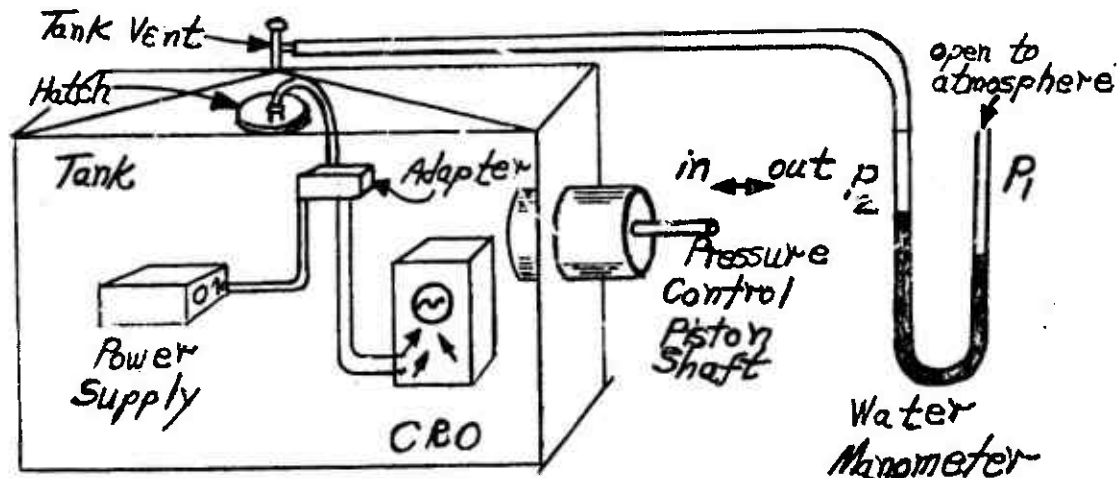


Figure 19. PITRAN Calibration Set-up

The electrical circuit is shown in figure 6-2.

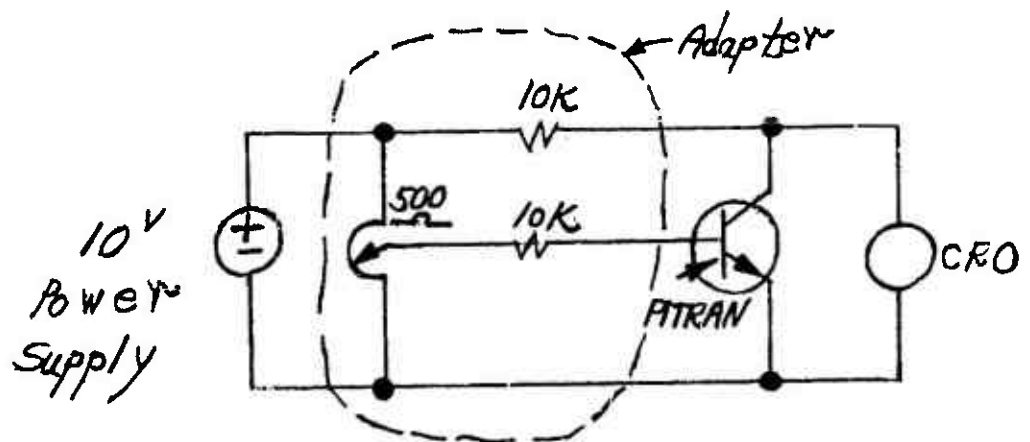


Figure 20. PITRAN Circuit



Sufficient air was retained in the top of the tank so that the pressure control piston could be fully inserted without forcing water out the tank vent and into the manometer. When the piston was withdrawn the water in the tank decreased, perhaps 2 inches, as air from the manometer tube entered the tank. This caused a change in hydrostatic pressure on the PITRAN of less than 0.1 psi. The calibration curves shown on figure 21, however, are based on the pressure measured by the manometer. Thus, it was assumed that changes in pressure at the tank vent were an adequate measure of changes in pressure at the PITRAN, and the 0.1 psi change due to tank level variation was neglected.

From figure 21, the PITRAN was found to have a calibration of 3.2 psi per volt (0.31 volts/psi) when  $V_{CE} = 1$  volt at zero differential pressure. The factory calibration was 1.73 psi per volt (0.58 volts/psi) with  $V_{CE} = 2$  volts. Stresses introduced into the transducer by the tank mounting hardware may have been responsible for the observed loss in sensitivity. Sufficient transducer sensitivity, however, was available to measure tank pressure as shown on figures 22 through 28 which were all recorded using a CRO set at 0.05 volts/cm on the vertical axis and 20 ms/cm on the horizontal axis. The vertical axis pressure calibration is therefore,  $3.2 \times 0.05 = 0.16$  psi/division.

Maximum amplitude of the piston periodic motion is possible only when the average position is near mid-stroke. Near either end of the stroke periodic motion is limited by the control system to avoid impact of the hydraulic piston with the ends of the cylinder, see p. 52 of reference 1. This "limiting" causes the difference between the traces on figure 25 and 27. The amplitude control setting was unchanged for the two conditions and the only difference was that the average piston control setting changed from 1/2 to 3/4 withdrawal, i.e., from 2.5 inches to 3.75 inches outward from full insertion.

One observed difficulty with the system was that two different amplitudes of motion occurred with the same amplitude control setting. For example, all control settings for figures 23 and 24 were the same but the system exhibited two modes of operation. The change from one piston motion amplitude to the other was abrupt and one mode appeared to be stable until the change to the other occurred. The same phenomena was observed in the change from figure 25 to 26. Neither mode of operation seemed to occur more often than the other.

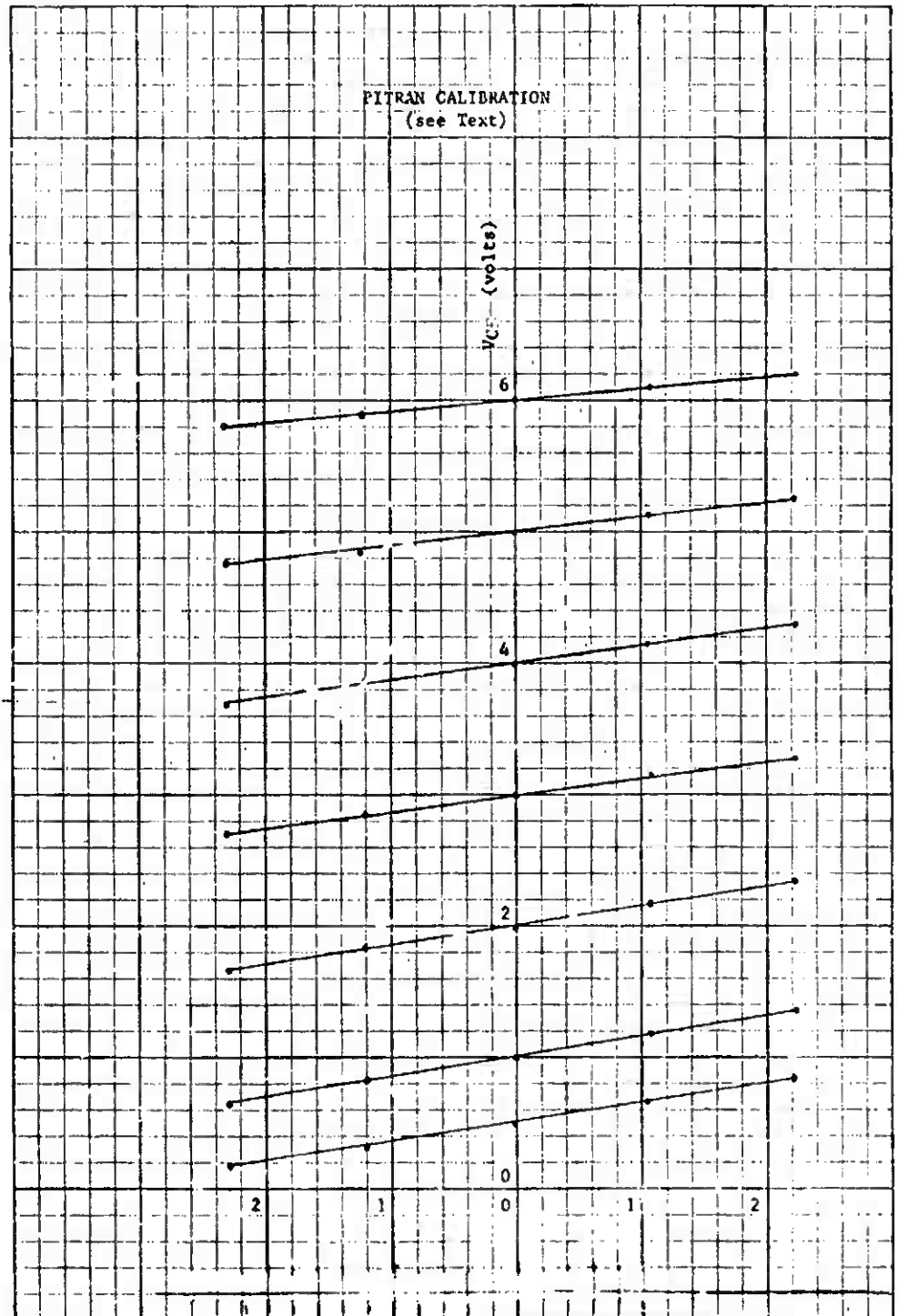


Figure 21. Tank Vent Pressure (psi)

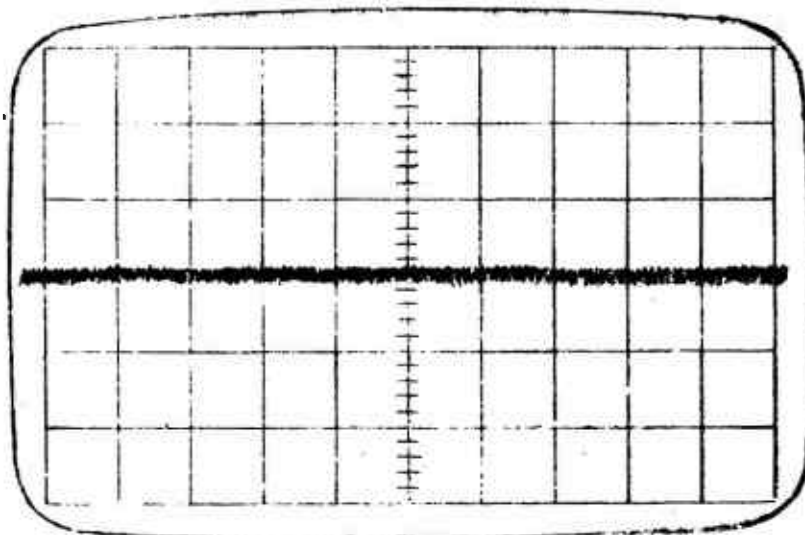


Figure 22 . Hydraulic Pump On. Average Piston Position: 1/2 Stroke. Piston Amplitude: 0.

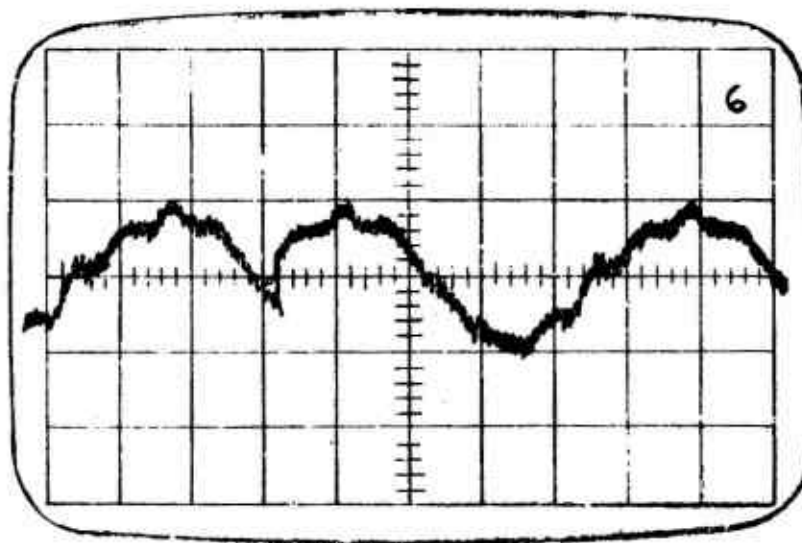


Figure 23. Average Piston Position: 1/2 Stroke. Piston Motion:  $\pm 0.25$  inch. Pressure Variation: 0.12 psi.  $f \approx 10.6$  cycles/sec.

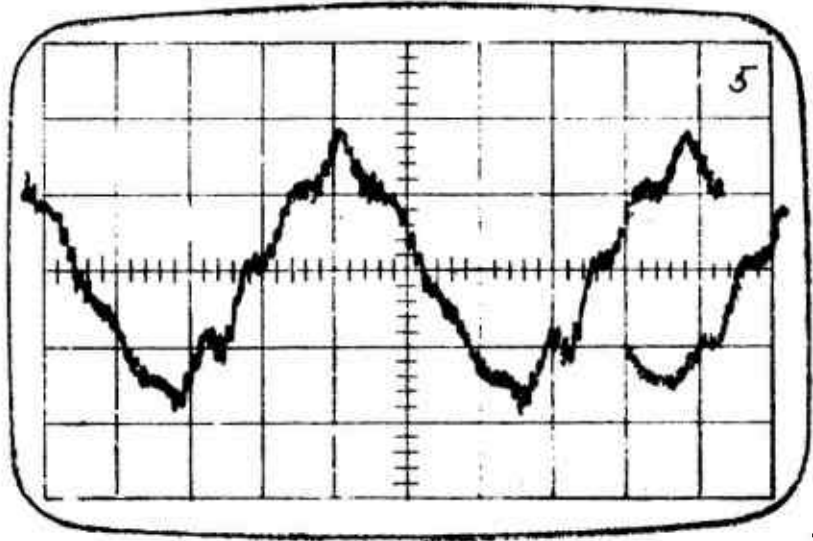


Figure 24. Average Piston Position: 1/2 Stroke. Piston Motion:  $\pm 0.5$  inch. Pressure Variation: 0.21 psi.  $f = 10.6$  cycles/sec.

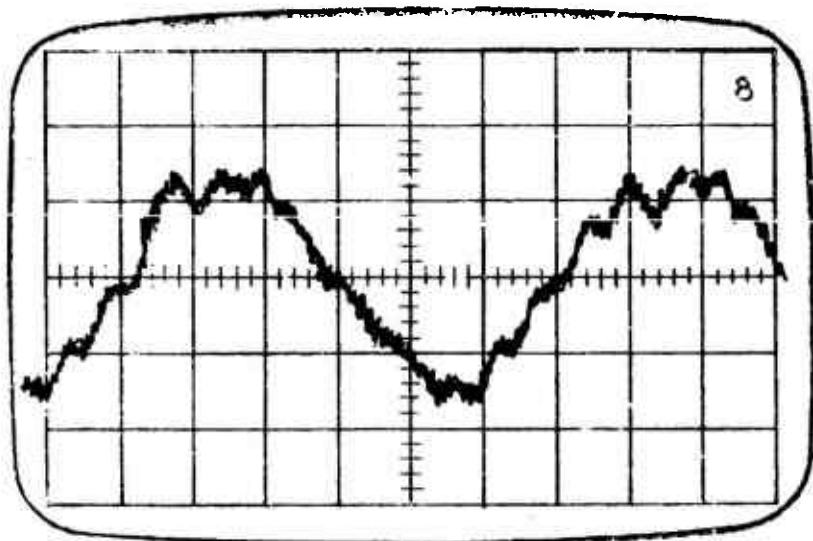


Figure 25. Average Piston Position: 1/2 Stroke. Piston Motion:  $\pm 0.28$  inch. Pressure Variation:  $\pm 0.21$  psi.  $f = 8$  cycles/sec.

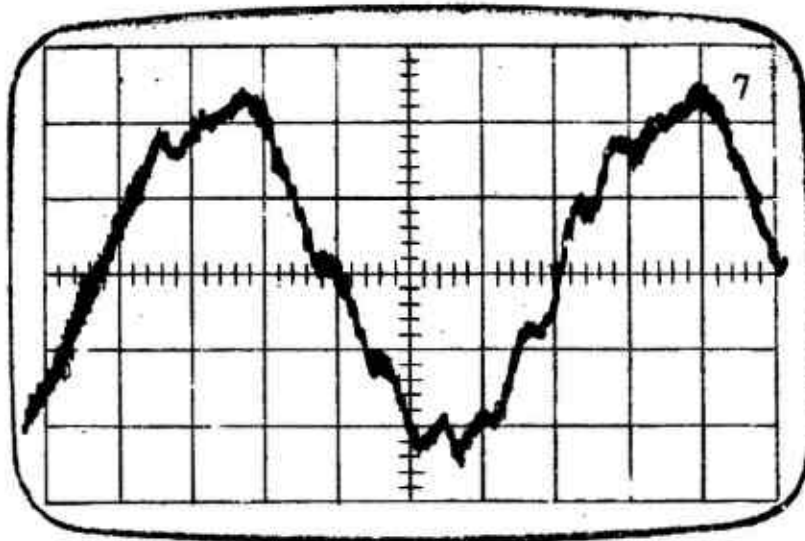


Figure 26. Average Piston Position: 1/2 Stroke. Piston Motion:  $\pm 0.56$  inch. Pressure Variation:  $\pm 0.37$  psi.  $f = 8$  cycles/sec.

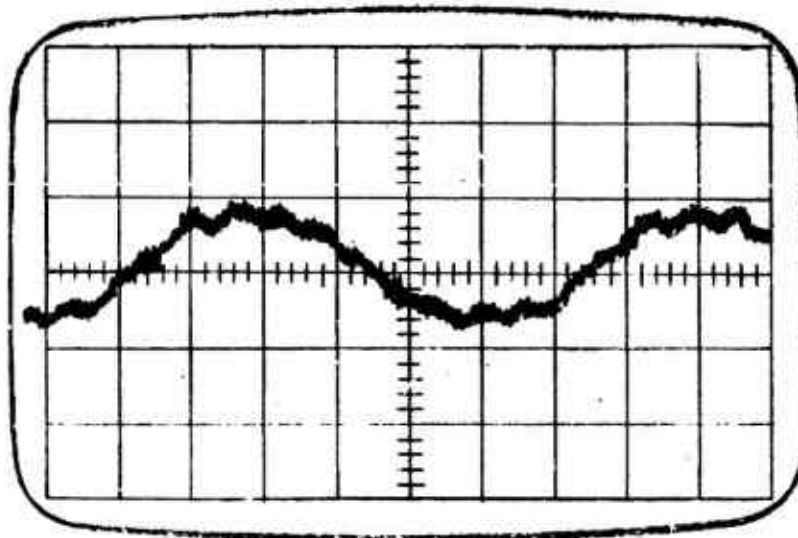


Figure 27. Average Piston Position: 3/4 Stroke (out). Piston Motion:  $\pm 0.16$  inch. Pressure Variation:  $\pm 0.09$  psi.  $f = 8$  cycles/sec.

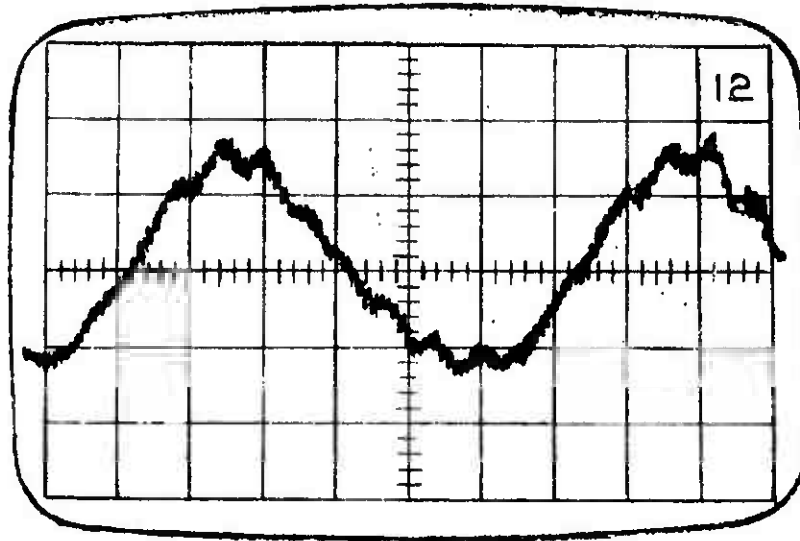


Figure 2d . Average Piston Position:  $3/4$  Stroke (out).  
 Piston Motion:  $\pm 0.34$  inch. Pressure Variation:  
 $\pm 0.22$  psi.  $f = 8$  cycles/sec.

## 6.2 Motor Thrust Measurement

Figure 29 is a photograph of a model pulse jet motor which was used to measure thrust. The motor had an air space of  $0.3 \text{ in}^3$  with a nozzle tube  $0.425 \text{ in.}$  long and  $1/16 \text{ in.}$  internal diameter. The model was attached to a stainless steel ball chain such as is often used for key chains. The chain weighed  $4.8 \text{ grams}$  in air and  $3.7 \text{ grams}$  in water. It was  $10 \text{ in.}$  long and was made up of 62 balls and links. Thus, in water, it required  $0.13 \times 10^{-3} \text{ lbf}$  to raise one ball

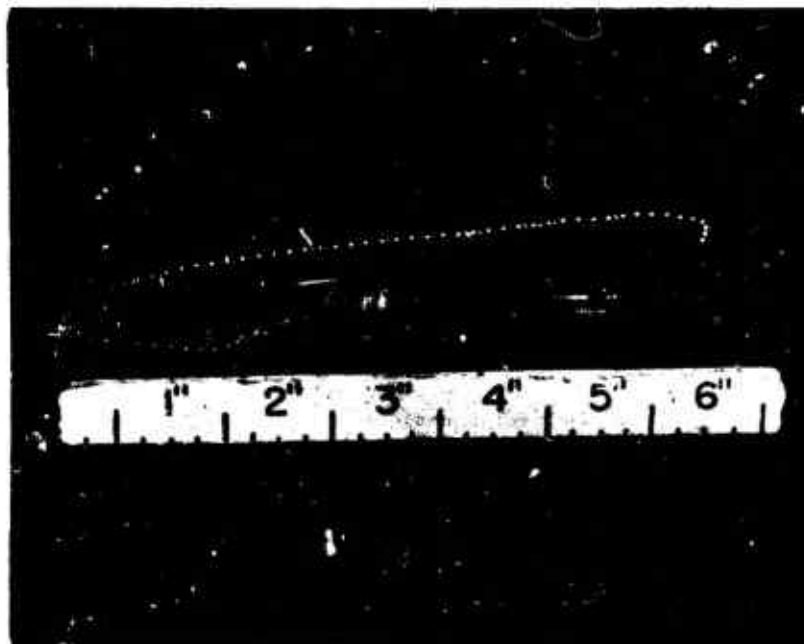


Figure 29. Thrust Model

from the tank floor. Measurements showed that at 11 hertz a pressure pulsation of  $0.32 \text{ psi}$  amplitude raised 2 balls, indicating that the motor was developing  $0.26 \times 10^{-3} \text{ lbf}$ . The thrust program included in the appendix yields a resonant frequency of 11.6 hertz and a thrust of  $0.25 \times 10^{-3} \text{ lbf}$  at the conditions used for the measurement. The agreement between experiment and theory was surprisingly good.

## 6.3 Model Velocity

A computation of expected model velocity was made based on the motor dimensions given on figure 6. The model was estimated to have a surface area of  $24 \text{ in}^2$  and a  $42^\circ$  angle between jet and model axes. The result was a prediction of  $1.8 \text{ ft/sec}$ , or  $22 \text{ in/sec}$ . At this velocity, the Reynold's Number was  $9.7 \times 10^4$ , the drag coefficient from the Blasius formula, see Eshbach - reference 3, page 6-37, was 0.00443, the dynamic pressure was  $3.14 \text{ lbf/ft}^2$ , and these conditions yield a computed drag of  $2.3 \times 10^{-3} \text{ lbf}$ .

At a frequency of 11.4 hertz and a pressure amplitude of  $0.37 \text{ lbf/in}^2$ , the thrusts from the port and starboard motors are equal at a value of

$1.56 \times 10^{-3}$  lbf. Thus, since  $\cos 42^\circ = 0.74$ , the total available thrust is computed to be  $2.3 \times 10^{-3}$  lbf.

Physical measurements of model velocity proved to be impossible because of the limited tank dimensions and the difficulty of maneuvering the model. The highest velocity actually observed by timing the model between two lines spaced one foot apart on the tank was 1/2 ft/sec. The model was accelerating and might have attained a steady-state velocity in the neighborhood of the computed 22 in/sec.



SECTION VII

CONCLUSIONS & SUGGESTIONS FOR FUTURE INVESTIGATIONS

A theory of operation of a Fluidic Pulse Jet Motor (FPJM) was developed which allows computation of motor thrust by means of a computer program. Excellent agreement was established between computed and measured thrust values.

A proposed design of a depth control system (DCS) was devised which should be applicable to any model using the Cartesian diver principle. Depth stability relations were developed and used to obtain a design criterion for a DCS.

Based on experience with the thrust measuring model, figure 29, a new model, figure 30, was designed which can be used to measure thrust with two alternate nozzles. The new model can also be used to verify the depth control system principle by adding a flexible rubber diaphragm above the upper end of the nozzle as shown in the figure.

It is recommended that the new design be built and used for thrust and depth stability measurements. Another worthwhile project will be to design and build a horizontally maneuverable model using a suitable depth control system. Following a successful demonstration of the latter device, a practical training device can be undertaken.

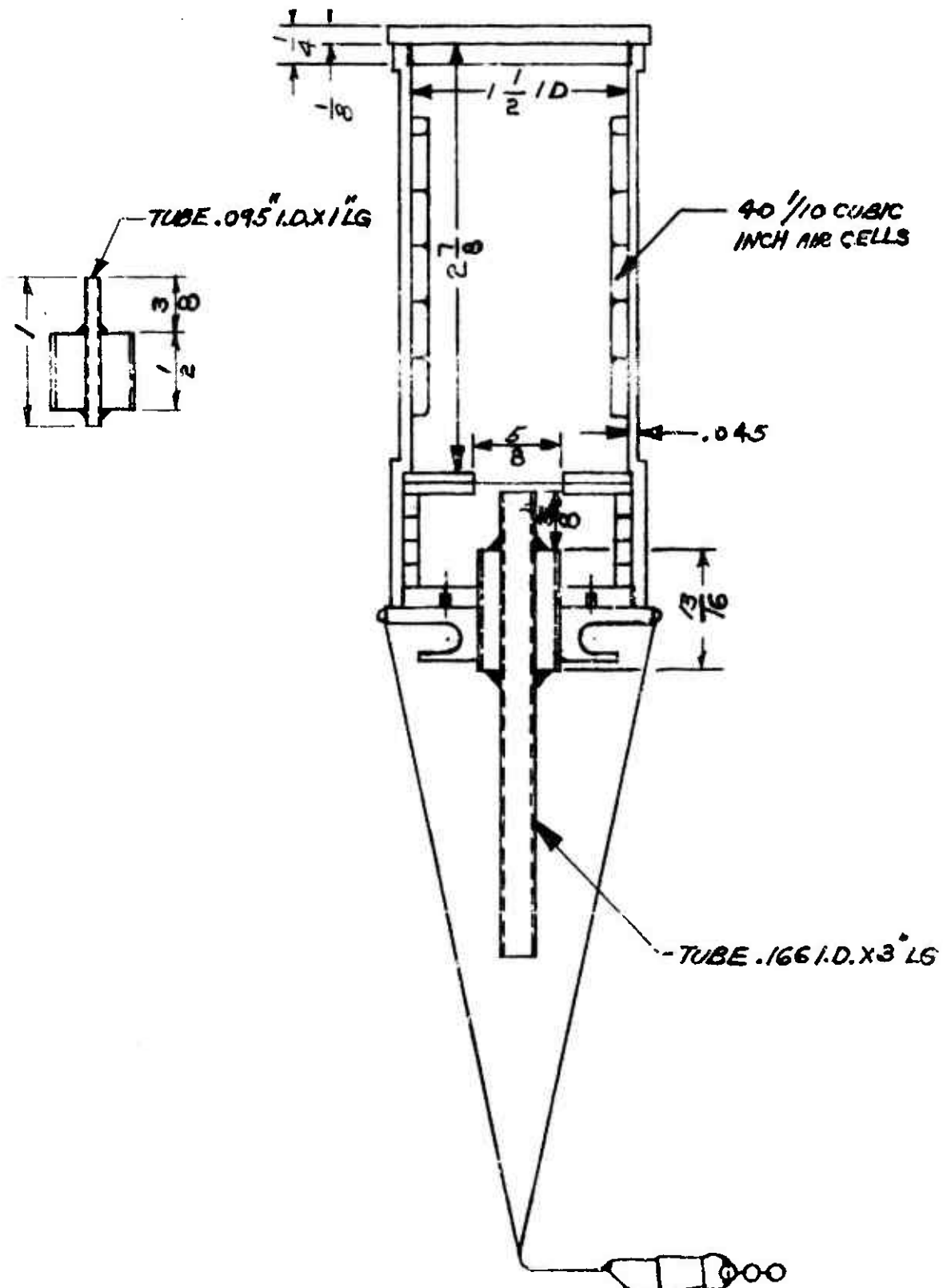


Figure 30. Thrust & Stability Model

REFERENCES

MOORE, L. R., and SOWERS, E. U., III; 3-D Display Program, Final Report, Contract N61339-69-C-0078, Bowles Fluidics Corporation, Silver Spring, Maryland, January, 1970.

KOCHENBURGER, R. J., "A Frequency Response Method for Analyzing and Synthesizing Contactor Servomechanisms," AIEE Transactions, Vol. 69, Part I, pp. 270-284, July 1950.

ESHBACH, O. W., Handbook of Engineering Fundamentals, John Wiley & Sons, New York, 1936.

## APPENDIX A

## PROGRAM FOR FLUIDIC PULSE JET MOTOR THRUST

PROGRAM TITLE				NUMBER
FLUIDIC PULSE JET MOTOR (FPJM) THRUST				N.A.
PROGRAM ABSTRACT				PROGRAMMED BY
COMPUTES THRUST, NATURAL FREQUENCY & SELECTIVITY (Q)				H. C. TOWLE
				DATE
				JULY 1970
BLOCKS				NO. OF STEPS
NO.	NO. OF STEPS	DATA REGISTERS	MARK USED	225
1	225	00-15	Mark 0,1	VERIFY NUMBER
				2391
				SET P.C. 000
				PAGE 1 of 7

1. Load the program tape, Depress REWIND; Depress RUN; TAPE REWIND; PRIME; LOAD PROGRAM; PRIME; LOAD PROGRAM (#2 program on tape).

2. PRIME; VERIFY PROGRAM; x register should read 2391.

3. SEARCH; Q. Computes, displays and stores

$\rho/g_c$  (lbm/in<sup>3</sup>). { y : + .935424078100 -04  
 $\rho$  -fluid density, lbm/in<sup>3</sup> { x : + .935424078100 -04  
 $g_c = 32.17 \div 12$ , dimensionless

---

$A = \frac{\pi D^2}{4}$

A - nozzle tube area in<sup>2</sup>.

D - nozzle tube diameter, in.

$\ell$  - nozzle tube length, in.

<p>4. Key <math>\ell</math>; <math>\uparrow</math>; D; <u>GO</u>.</p> <p>Read y : A x : 4</p>	<p><u>EXAMPLE</u></p> <p>0.425; <math>\uparrow</math>; .0625; <u>GO</u></p> <p>y: + .306796157575 -02 x: + 4.00...</p>
---	--

## PROGRAM TITLE

FLUIDIC PULSE JET MOTOR (FPJM) THRUST

PAGE 2 of 9

$$L = \frac{\rho \ell}{8c}$$

$$C = \frac{V}{nAp}$$

$$N \approx \frac{8P}{3\pi 8c} \left[ 1 + 2C_D \frac{\ell}{D} \right] = \frac{R}{|U|}$$

$$f_0 = \frac{1}{2\pi \sqrt{LC}}$$

C - equivalent capacitance, in<sup>3</sup>/lb<sup>2</sup>.

C<sub>D</sub> - drag coefficient, assumed = 0.01, dimensionless.

f<sub>0</sub> - undamped natural frequency, cycles/aec.

L - equivalent inductance, lbm/in<sup>2</sup>.

N - as defined above, lbm/in<sup>3</sup>.

p - average motor chamber pressure, lbf/in<sup>2</sup>.

R - equivalent resistance, lbm/in<sup>2</sup> - aec.

|U| - amplitude of sinusoidal jet velocity, ft/sec.

5. Key V; GO

Read y: f<sub>0</sub>  
 x: 1/f<sub>0</sub>  
 005: L  
 006: C  
 007: N

## EXAMPLE (continued)

Key 0.393; GO

Read y: + 10.1174895006  
 x: + .988387484799 -01  
 005: + .397555233192 -04  
 006: + 6.22439670150  
 007: + .901998334297 -04

$$F_0 = \frac{3\pi AP}{32 \left[ 1 + 2C_D \frac{\ell}{D} \right]}$$

F<sub>0</sub> - motor average thrust at resonance, lbf.

P - amplitude of sinusoidal change of pressure in surrounding fluid, lbf/in<sup>2</sup>.

PROGRAM TITLE	
FLUIDIC PULSE JET MOTOR (FPJM) THRUST	PAGE 3 of 9
6. Key <u>P</u> ; <u>GO</u>  Read y: Fo x: P	EXAMPLE (continued) Key <u>.9018</u> ; <u>GO</u>  Read y: + .717303524457 -03 x: + .901800...
$ U ^2 = \frac{-b + \sqrt{b^2 - 4ac}}{2a}$ $F = \frac{PA}{4g_c}  U ^2$ $Q = \frac{\omega_o L}{R}$ $a = N^2$ $b = [\omega L - 1/\omega C]^2$ $c = -p^2$ <p>F - average thrust of motor, lbf.</p> <p>f - frequency of sinusoidal change of pressure in surrounding fluid, cycles/sec.</p> <p>Q - selectivity, dimensionless</p> $\omega = 2\pi f; \omega_o = 2\pi f_o$	
7. Key <u>f</u> ; <u>GO</u>  Read y: F x: f 013:  U ^2 014: Q	EXAMPLE (continued) Key <u>5</u> ; <u>GO</u>  Read y: +.654457482480 -03 x: +5.000... 013: +9121.85087551 014: +.293361343431
8,9,... Repeat Step 7 for all desired values of f.	EXAMPLE (continued) Key <u>20</u> ; <u>GO</u>  Read y: +.658967612802 -03 x: +20.00... 013: +9184.57384655 014: +.292357920840

## NAVTRAEQUIPCEN IH-187

Step	Key	Code	Comment	Display		Storage Register	
				X	Y	No.	Contents
00 0	MARK	0403	SEARCH 0	0	0		
1	0	0700	COMPUTE				
2	6	0706	$\rho / g_c$				
3	2	0702					
4	.	0712					
5	4	0704		62.4			
6	$\uparrow$	0604			62.4		
7	3	0703					
8	2	0702					
9	.	0712					
010	1	0701					
11	7	0707		32.17			
12	$\div$	0603			62.4/32.17		
13	1	0701					
14	2	0702		12			
15	$x^2$	0713		$12^2$			
16	$x^2$	0713		$12^4$			
17	$\div$	0603	$\rho / g_c$		$\rho / g_c$		
18	$\downarrow$	0605	DISPLAY	$\rho / g_c$			
19	STORE Y	0414					
020	000	0000				000	$\rho / g_c$
21	STOP	0515	ENTER $\ell, D$				
22	STORE Y	0414	STORE	D	$\ell$		
23	001	0001	DATA			001	$\ell$
24	ST DIR	0404					
25	002	0002				002	D
26	$x^2$	0713	COMPUTE	$D^2$			
27	$\uparrow$	0604	AREA		$D^2$		
28	$\pi$	0609		$\pi$			
29	x	0602			$\pi D^2$		
30	4	0704		4			
31	$\div$	0603	A		A		
32	STORE Y	0414					
33	003	0003				003	A
34	STOP	0515	ENTER V	4	A		
35	ST DIR	0404	COMPUTE	V			
36	004	0004	L			004	V
37	RECALL Y	0415					
38	000	0000			$\rho / g_c$		
39	RE DIR	0405					

## NAVTRAEQUIPCEN IH-187

Step	Key	Code	Comment	Display		No.	Storage Register Contents
				X	Y		
040	001	0001		$\ell$	$\rho/\rho_c$		
41	x	0602	$\rho^2/\rho_c = L$		L		
42	STORE Y	0414					
43	005	0005				005	L
44	RECALL Y	0414	COMPUTE				
45	004	0004	C		V		
46	RE DIR	0405					
47	003	0003		A			
048	$\div$	0603			V/A		
49	1	0701					
050	4	0704					
51	.	0712					
52	7	0707	$\rho$ (average)	14.7			
53	$\div$	0603			V/Ap		
4	1	0701					
55	.	0712					
56	4	0704	n	1.4			
57	$\div$	0603	$V/nAp = C$		C		
58	STORE y	0414					
59	006	0006				006	C
060	.	0712	COMPUTE				
61	0	0700	N				
62	2	0702	$2C_D = 0.02$	0.02			
63	$\uparrow$	0604			0.02		
64	RE DIR	0405					
65	001	0001		$\ell$			
66	x	0602			$0.02 \ell$		
67	RE DIR	0405					
68	002	0002		D			
69	$\div$	0603	$2C_D (\ell/D)$		$0.2 \ell/D$		
070	1	0701					
71	+	0600	$1 + 2C_D (\ell/L)$		$1 + 2C_D \ell/D$		
072	STORE y	0414					
73	015	0015				015	$1 + 2C_D \ell/D$
74	RE DIR	0405					
75	000	0000		$\rho/\rho_c$			
76	x	0602			$3\rho/N\delta$		
77	8	0708		8			
78	x	0602			$3\rho/N$		
79	2	0702					



## NAVTRAEQUIPCEN IH-187

Step	Key	Code	Comment	Display		Storage Register	
				X	Y	No.	Contents
080	$\div$	0603		3	$\pi/N$		
81	$\pi$	0609		$\pi$			
82	$\div$	0603			N		
83	STORE Y	0414					
84	007	0007				007	N
85	RECALL Y	0415	COMPUTE				
86	005	0005	$f_0$		L		
87	RE DIR	0405					
88	006	0006		C			
89	x	0602			LC		
090	$\downarrow$	0605		LC			
91	$\sqrt{x}$	0612		$\sqrt{LC}$			
92	$\uparrow$	0604			$\sqrt{LC}$		
93	2	0702		2			
94	x	0602			$2\sqrt{LC}$		
95	$\pi$	0609		$\pi$			
096	x	0602			$2\pi\sqrt{LC}$		
97	1	0701		1			
98	( )	0606		$2\pi\sqrt{LC}$	1		
99	$\div$	0603	$f_0$	$2\pi\sqrt{LC}$	$f_0$		
100	SIGNAL X	0414					
101	008	0008				008	$f_0$
102	STOP	0515	ENTER P	$1/f_0$	$f_0$		
103	ST DIR	0404	COMPUTE	P			
104	009	0009	$F_0$			009	P
105	$\uparrow$	0604			P		
106	RE DIR	0405					
107	003	0003		A			
108	x	0602			AP		
109	$\pi$	0609		$\pi$			
110	x	0602			$\pi AP$		
111	3	0703		3			
112	x	0602			$3\pi AP$		
113	3	0703					
114	2	0702		32			
115	$\div$	0603			$3\pi AP/32$		
116	RE DIR	0405					
117	015	0015		$1 + 2C_0^{1/2}/D$			
118	$\div$	0603	$F_0$		$F_0$		
119	STORE Y	0414					



Step	Key	Code	Comment	Display		No.	Storage Register Contents
				X	Y		
120	010	0010		$1+2C_D \frac{L}{D}$	$F_0$	010	$F_0$
121	RE DIR	0105	DISPLAY				
122	009	0009		P	$F_0$		
123	MARK	0403					
124	1	0701					
125	STOP	0515	ENTER f	P	$F_0$		
126	ST DIR	0404	COMPUTE	f			
127	011	0011	$ U ^2$			011	f
128	↑	0404			f		
129	2	0702		2			
130	x	0602			2f		
131	π	0609		π			
132	x	0702	$\omega = 2\pi f$		$\omega$		
133	STORE Y	0414					
134	014	0014				014	$\omega$
135	RE DIR	0405					
136	005	0005		L			
137	x	0602			$\omega L$		
138	STORE Y	0414					
139	013	0013				013	$\omega L$
140	1	0701		1			
141	↑	0404			1		
142	RE DIR	0405					
143	006	0006		C			
144	$\frac{1}{C}$	0603			$1/C$		
145	RE DIR	0405					
146	014	0014		$\omega$			
147	$\frac{1}{C}$	0603			$1/\omega C$		
148	↑	0605		$1/\omega C$			
149	- DIR	0401					
150	013	0013				013	$\omega L - 1/\omega C$
151	RE DIR	0105					
152	013	0013		$\omega L - 1/\omega C$			
153	$x^2$	0713	$\frac{1}{4}(\omega L - 1/\omega C)^2$	b			
154	$x^2$	0713		$b^2$			
155	ST DIR	0404					
156	012	0012				012	$b^2$
157	RE DIR	0105					
158	009	0009		P			
159							

## NAVTRAEQUIPCEN IH-187

Step	Key	Code	Comment	Display		Storage Register	
				X	Y	No.	Contents
160	↑	0604		-c	-c		
161	RE DIR	0605					
162	007	0007		N			
163	X <sup>2</sup>	0713	$a = N^2$	a			
164	X	0602			-ac		
165	4	0704		4			
166	x	0602			-4ac		
167	↓	0605		-4ac			
168	+ DIR	0600					
169	012	0012				012	$b^2 - 4ac$
170	RE DIR	0605					
171	012	0012		$b^2 - 4ac$			
172	$\sqrt{x}$	0.12	$r = \sqrt{b^2 - 4ac}$	r			
173	ST DIR	0404					
174	012	0012				012	r
175	RE DIR	0605					
176	013	0013		$\sqrt{b}$			
177	X <sup>2</sup>	0713		b			
178	- DIR	0401					
179	012	0012				012	$-b + r$
180	2	0602		2			
181	↑	0604			2		
182	RE DIR	0605					
183	007	0007		N			
184	X <sup>2</sup>	0713		a			
185	X	0602			2a		
186	↓	0605		2a			
187	RECALL Y	0415					
188	012	0012			$-b + r$		
189	÷	0603	$ u ^2$		$ u ^2$		
190	STORE Y	0414					
191	013	0013				013	$ u ^2$
192	RECALL Y	0415	COMPUTE				
193	008	0008	Q		$f_0$		
194	2	0702		2			
195	x	0602			$2f_0$		
196	$\pi$	0609		$\pi$			
197	x	0602	$\Delta' = 2\pi f_0$		$\Delta_0$		
198	RE DIR	0605					
199	005	0005		1			

Step	Key	Code	Comment	Display		Storage Register	
				X	Y	No.	Contents
20 0	x	0'02		L	$\omega_0 L$		
20 1	RE DIR	0'05					
20 2	007	0007		N			
20 3	$\div$	0'03			$\omega_0 L/N$		
20 4	RE DIR	0'05					
20 5	013	0013		$ U ^2$			
20 6	$\sqrt{x}$	0'12		$ U $			
20 7	$\div$	0'05	$C = \omega_0 L/N U $		Q		
20 8	STORE Y	0'14					
20 9	014	0014				014	Q
21 0	$x^2$	0'24	COMPLETE	$ U ^2$			
21 1	$\uparrow$	0'05	THRUST		$ U ^2$		
21 2	RC DIR	0'05	(F)				
21 3	000	0000		$S/S_c$			
21 4	x	0'02			$S U ^2/S_c$		
21 5	RC DIR	0'05					
21 6	003	0003		A			
21 7	x	0'02			$S_h U ^2/S_c$		
21 8	4	0'04		4			
21 9	$\div$	0'03	$F = S_h U ^2/S_c$		F		
22 0	RC DIR	0'05					
22 1	011	0011	DISPLAY	F			
22 2	SEARCH	0'07					
22 3	1	0701	TO 125				
22 4	END PROG	0512					
5							
6							
7							
8							
9							
0							
1							
2							
3							
4							
5							
6							
7							
8							
9							

## 700 PROGRAM CODES

CODE	KEY	CODE	KEY
0400	+ DIRECT	0600	+
0401	- DIRECT	0601	-
0402	x DIRECT	0602	x
0403	÷ DIRECT	0603	÷
0404	STORE DIRECT	0604	↑
0405	RECALL DIRECT	0605	↓
0406	 DIRECT	0606	( )
0407	SEARCH	0607	X
0408	MARK	0608	INTEGER X
0409	GROUP 1	0609	$\pi$
0410	GROUP 2	0610	$\text{Log}_{10} X$
0411	WRITE	0611	$\text{Log}_e X$
0412	WRITE ALPHA	0612	$\sqrt{X}$
0413	END ALPHA	0613	$10^x$
0414	STORE Y*	0614	$e^x$
0415	RECALL Y*	0615	$\frac{1}{x}$
0500	+ INDIR	0700	0
0501	- INDIR	0701	1
0502	x INDIR	0702	2
0503	÷ INDIR	0703	3
0504	STORE INDIR	0704	4
0505	RECALL INDIR	0705	5
0506	 INDIR	0706	6
0507	SKIP if $Y \geq X$	0707	7
0508	SKIP if $Y < X$	0708	8
0509	SKIP if $Y = X$	0709	9
0510	SKIP if ERROR	0710	SET EXP
0511	RETURN	0711	CHANGE SIGN
0512	END PROG	0712	DECIMAL POINT
0513	LOAD PROG	0713	$x^2$
0514	GO	0714	RECALL RESIDUE
0515	STOP	0715	CLEAR X

\*ENTERED BY TOGGLE SWITCHES